

## Molecular imaging of thyroid and parathyroid diseases

Petra Petranović Ovčariček, Letizia Calderoni, Alfredo Campenni, Stefano Fanti & Luca Giovanella

To cite this article: Petra Petranović Ovčariček, Letizia Calderoni, Alfredo Campenni, Stefano Fanti & Luca Giovanella (2024) Molecular imaging of thyroid and parathyroid diseases, Expert Review of Endocrinology & Metabolism, 19:4, 317-333, DOI: [10.1080/17446651.2024.2365776](https://doi.org/10.1080/17446651.2024.2365776)

To link to this article: <https://doi.org/10.1080/17446651.2024.2365776>



© 2024 The Author(s). Published by Informa UK Limited, trading as Taylor & Francis Group.



Published online: 18 Jun 2024.



Submit your article to this journal [↗](#)



Article views: 1400



View related articles [↗](#)



View Crossmark data [↗](#)

## Molecular imaging of thyroid and parathyroid diseases

Petra Petranović Ovcariček<sup>a,b</sup>, Letizia Calderoni<sup>c,d</sup>, Alfredo Campenni<sup>e</sup>, Stefano Fanti<sup>c,d</sup> and Luca Giovanella<sup>f,g</sup>

<sup>a</sup>Department of Oncology and Nuclear Medicine, University Hospital Center Sestre Milosrdnice, Zagreb, Croatia; <sup>b</sup>School of Medicine, University of Zagreb, Zagreb, Croatia; <sup>c</sup>Nuclear Medicine Division, IRCCS Azienda Ospedaliero-Universitaria di Bologna, Policlinico S. Orsola, Bologna, Italy; <sup>d</sup>Nuclear Medicine, Alma Mater Studiorum, University of Bologna, Bologna, Italy; <sup>e</sup>Department of Biomedical and Dental Sciences and Morpho-Functional Imaging, Unit of Nuclear Medicine, University of Messina, Messina, Italy; <sup>f</sup>Department of Nuclear Medicine, Gruppo Ospedaliero Moncucco, Lugano, Switzerland; <sup>g</sup>Clinic for Nuclear Medicine, University Hospital of Zürich, Zürich, Switzerland

### ABSTRACT

**Introduction:** Molecular imaging of thyroid and parathyroid diseases has changed in recent years due to the introduction of new radiopharmaceuticals and new imaging techniques. Accordingly, we provided an clinicians-oriented overview of such techniques and their indications.

**Areas covered:** A review of the literature was performed in the PubMed, Web of Science, and Scopus without time or language restrictions through the use of one or more fitting search criteria and terms as well as through screening of references in relevant selected papers. Literature up to and including December 2023 was included. Screening of titles/abstracts and removal of duplicates was performed and the full texts of the remaining potentially relevant articles were retrieved and reviewed.

**Expert opinion:** Thyroid and parathyroid scintigraphy remains integral in patients with thyrotoxicosis, thyroid nodules, differentiated thyroid cancer and, respectively, hyperparathyroidism. In the last years positron-emission tomography with different tracers emerged as a more accurate alternative in evaluating indeterminate thyroid nodules [<sup>18</sup>F-fluorodeoxyglucose (FDG)], differentiated thyroid cancer [<sup>124</sup>I-iodide, <sup>18</sup>F-tetrafluoroborate, <sup>18</sup>F-FDG] and hyperparathyroidism [18F-fluorocholine]. Other PET tracers are useful in evaluating relapsing/advanced forms of medullary thyroid cancer (<sup>18</sup>F-FDOPA) and selecting patients with advanced follicular and medullary thyroid cancers for theranostic treatments (<sup>68</sup>Ga/<sup>177</sup>Ga-somatostatin analogues).

### ARTICLE HISTORY

Received 24 March 2024  
Accepted 5 June 2024

### KEYWORDS

Thyroid scintigraphy; radioiodine; differentiated thyroid cancer; benign thyroid diseases; [<sup>18</sup>F]-fluorodeoxyglucose; hyperparathyroidism; [<sup>99m</sup>Tc] Tc-MIBI; choline

## 1. Introduction

Radioiodine uptake test and thyroid scintigraphy are widely used methods to evaluate morpho-functional aspects of the thyroid gland. Immunometric assays, multiparametric thyroid ultrasound (US), and fine needle aspiration cytology (FNAC) contribute to thyroid evaluation in clinical practice. However, thyroid scintigraphy remains the only technique able to: a. differentiate “productive” from “destructive” thyrotoxicosis and b. detect autonomously functioning nodules (AFTNs). Finally, the thyroid scan can be also quantified, both via measuring the uptake and the spatial distribution of the radiopharmaceutical within the thyroid gland. Additionally, different radiotracers able to evaluate the metabolism and proliferation rate of “cold” thyroid nodules can be interrogated on the malignancy rate of cytologically indeterminate “cold” nodules and reduce unnecessary diagnostic lobectomies/thyroidectomies. Whole-body imaging with radioiodine is integral in theranostic management of patients with DTC. Moreover, PET is relevant in managing patients with either DTC ([<sup>18</sup>F]-FDG, Iodine-124) or MTC ([<sup>18</sup>F]FDOPA, [<sup>18</sup>F]-FDG). Scintigraphy with [<sup>99m</sup>Tc]Tc-MIBI is the standard of care in localizing hyperfunctioning parathyroids glands before surgery but [<sup>18</sup>F]FCH recently demonstrated to be the best one-stop-shop method

for this purpose and is rapidly substituting conventional scintigraphy. Finally, new radiopharmaceuticals are currently under evaluation and radiomic analysis of functional imaging data is emerging as a potential game-changer, especially in patients with thyroid cancers. The aim of our paper is to summarize molecular imaging methods available for thyroid and parathyroid evaluation, provide practical suggestions for their optimized use in clinical practice, and discuss perspectives in the field.

## 2. Thyroid and parathyroid radiopharmaceuticals

### 2.1. Gamma-emitting radiopharmaceuticals

#### 2.1.1. Tracing follicular thyroid cells' function

Radioiodine or Na[<sup>131</sup>I] (<sup>131</sup>I) is actively transported into the thyroid via the Na<sup>+</sup>/I<sup>-</sup> symporter (NIS), a key plasma membrane glycoprotein, which is located on the basolateral membrane of thyroid cells [1]. The radionuclide <sup>131</sup>I is in fact the first theragnostic radiopharmaceutical. It decays with β-electron and gamma photon emission. Its gamma photon emission enables diagnostic imaging to quantify the distribution and kinetics of iodine in the thyroid gland, while β-particle emission is used for therapeutic purposes [2]. <sup>131</sup>I and its analogues

### Article highlights

- Molecular imaging is key for the diagnosis and management of thyroid and parathyroid diseases.
- Thyroid scintigraphy is pivotal in detecting autonomously functioning thyroid nodules (AFTN) and may support the differential diagnosis of cytologically indeterminate nodules. Radioiodine scintigraphy remains central to stage, restage, and monitor patients with differentiated thyroid cancers treated with radioiodine. Planar and whole-body scintigraphy should be complemented with SPECT/CT whenever possible to increase diagnostic accuracy.
- PET/CT with different tracers is used for disease staging and to assess disease recurrence of both follicular thyroid cell-derived tumors ( $^{18}\text{F}$ -FDG) and MTC ( $^{18}\text{F}$ FDOPA and  $^{18}\text{F}$ -FDG).
- PET/CT with  $^{68}\text{Ga}$ -SSA is increasingly employed to select patients with advanced DTC and MTC patients for subsequent  $^{177}\text{Lu}$ -SSA therapy (theranostic approach).
- Parathyroid scintigraphy and SPECT/CT with  $^{99\text{m}}\text{Tc}$ -MIBI and PET/CT with  $^{18}\text{F}$ JFCH can be used as imaging modality in patients with hyperparathyroidism. The latter shows superior accuracy and is now proposed as a one-stop-shop first-line procedure, whenever possible.

isotopes are actively transported into the thyroid via the NIS, as well as  $\text{Na}^{99\text{m}}\text{TcTcO}_4$  due to similar stoichiometric characteristics [3]. The  $\text{Na}^{99\text{m}}\text{TcTcO}_4$  is similar to the iodide ion in mass, size, and charge density, but unlike iodide once internalized it does not undergo organification and therefore does not participate in thyroid hormone synthesis [4]. The process of extracting these ions from plasma and concentrating them within thyroid cells represents active and saturable activity. Therefore,  $\text{Na}^{99\text{m}}\text{TcTcO}_4$  and iodide compete for NIS by being simultaneously transported from the extracellular space [5]. In benign thyroid disease, the use of  $\text{Na}^{99\text{m}}\text{TcTcO}_4$  is preferred because it is widely available, has more favorable dosimetry and is relatively inexpensive.

### 2.1.2. Tracing follicular thyroid and/or parathyroid cells' proliferation

$^{99\text{m}}\text{Tc}$ -Methoxy-IsoButyl-Isonitrol ( $^{99\text{m}}\text{Tc}$ -MIBI) is a lipophilic radiopharmaceutical with a central technetium atom positively charged bound to six ligands. After intravenous administration,  $^{99\text{m}}\text{Tc}$ -MIBI penetrates reversibly into the cytoplasm through thermodynamic driving forces and then irreversibly crosses the mitochondrial membrane using a different membrane potential gradient through the cell and mitochondrial membrane layers [6].  $^{99\text{m}}\text{Tc}$ -MIBI is then rapidly eliminated from the blood, concentrating in salivary glands and thyroid glands, as well as in muscles, liver, and kidneys [7]. Cancer cells, due to their high metabolic turnover, are characterized by high electrical gradients of the mitochondrial membrane and demonstrate greater accumulation compared to healthy cells. The final concentration of the lesion is generally proportional to the blood flow to the tissue and the duration of blood retention. Initially developed as a myocardial perfusion agent,  $^{99\text{m}}\text{Tc}$ -MIBI has later been shown to nonspecifically localize in a variety of malignant and nonmalignant tumors [8]. In 1989 and subsequent years, localization of  $^{99\text{m}}\text{Tc}$ -MIBI in parathyroid and thyroid adenomas [9,10]. The peak activity of  $^{99\text{m}}\text{Tc}$ -MIBI occurs several minutes after injection in both thyroid and parathyroid tissue.

However, while the activity in the thyroid decreases over time, it remains in parathyroid tissue.  $^{99\text{m}}\text{Tc}$ -MIBI demonstrates a favorable thyroid/parathyroid ratio, but its uptake in adenomas and parathyroid hyperplasia varies. Sensitivity for adenomas is slightly higher than for hyperplasia, though statistically significant [11]. The size of the parathyroid gland generally correlates with PTH secretion. However, scintigraphy's positivity in localizing adenomas is strongly associated with the degree of oxyphilic cellularity than with size. This correlation is likely due to the abundance of mitochondria in oxyphilic cells and their high metabolic activity. Consequently, some large adenomas lacking oxyphilic cells may not exhibit tracer uptake as well as cystic adenomas [12].

## 2.2. Positron-emitting radiopharmaceuticals

### 2.2.1. $^{18}\text{F}$ -fluorodeoxyglucose

$^{18}\text{F}$ FDG is a synthetic, positron-emitting glucose analog, specifically formulated for use in PET.  $^{18}\text{F}$ FDG emulates the behavior of glucose by using glucose transporters (GLUTs) to actively penetrate cell membranes. This process involves a competitive interaction with endogenous glucose, as both substances compete for uptake into cells. Administered intravenously,  $^{18}\text{F}$ FDG rapidly permeates body fluids, accessing different tissues through GLUTs and subsequently being sequestered within cellular structures, since it is not then further metabolized in the glucose pathway [13,14]. The distribution of  $^{18}\text{F}$ FDG in tumor tissues is directly related to blood flow. Facilitated diffusion, predominantly facilitated by specific glucose transporters such as GLUT-1, is the main mechanism by which the radiotracer enters cells. In particular, high levels of GLUT-1 are intimately linked to increased uptake of  $^{18}\text{F}$ FDG in human tumors. Furthermore, increased GLUT-1 expression serves as a relevant marker for hypoxia, indicating insufficient vascular support to meet local metabolic demands in the tumor microenvironment [15,16]. The distinctive attribute of  $^{18}\text{F}$ FDG is its ability to mirror glucose metabolism, offering valuable insights into tissue metabolic activity. This inherent feature makes  $^{18}\text{F}$ FDG an indispensable tool in oncologic imaging, facilitating the identification of regions of altered metabolic needs. By providing a dynamic view of glucose utilization,  $^{18}\text{F}$ FDG contributes significantly to our understanding of the metabolic nuances of various tissues, enhancing our ability to characterize and diagnose pathological conditions, especially in the field of oncology [17].

### 2.2.2. $^{124}\text{I}$ -sodium iodide

This isotope shares identical biochemical behavior with other iodine isotopes, combining tracer specificity with the high resolution of PET/CT. The enhanced sensitivity and spatial resolution of PET/CT, compared to standard gamma scintigraphy, facilitate the detection of recurrent or metastatic disease and enable more precise measurements of metabolic tumor volumes [18].

In recent years, there has been a growing interest in  $^{18}\text{F}$  tetrafluoroborate ( $^{18}\text{F}$ TFB) as a promising radiopharmaceutical for PET imaging, serving as another iodide analog. Unlike radioiodide,  $^{18}\text{F}$ TFB does not undergo organification in thyroid cells, offering the advantage of relatively lower uptake in healthy thyroid tissue. Initial clinical trials involving  $^{18}\text{F}$ TFB have been conducted on both healthy human subjects and

patients with thyroid cancer. The outstanding imaging characteristics of [ $^{18}\text{F}$ ]TfR for assessing tissues expressing NIS point toward its promising future in NIS PET imaging [19]. Notably, however, [ $^{18}\text{F}$ ]TfR is not approved for clinical use and its use is currently restricted to clinical trials.

### 2.2.3. [ $^{11}\text{C}$ ] and [ $^{18}\text{F}$ ]-labeled choline analogues

Choline is an indispensable component in numerous biological pathways and plays a central role in several cellular processes. It is involved in the biosynthesis of integral cell membrane phospholipids, methyl metabolism, cholinergic neurotransmission, transmembrane signaling, lipid, and cholesterol transport, and metabolism. In the context of PET imaging, choline-based tracers serve as substrates for phospholipid synthesis, offering a unique perspective on cellular activity [20]. In the field of cancer biology, the importance of choline becomes particularly apparent. Cancer cells, characterized by rapid duplication of the cell membrane due to hyperactivity of choline kinase enzymes, show an increased demand for choline. This increased choline utilization is manifested by elevated levels of choline and phosphatidylcholine in tumor cells, reflecting increased choline uptake and phosphorylation. In less proliferative tumors, changes in choline transport, incorporation, and utilization result in elevated levels of phospholipid metabolites [21]. The biochemical resemblance of [ $^{11}\text{C}$ ]choline to endogenous choline positions it as a widely employed PET/CT imaging agent, particularly in cases where the GLUT system is not overexpressed. Physiological uptake of [ $^{11}\text{C}$ ]choline is observable in various glands (pituitary, salivary glands, pancreas) and organs (liver, kidney, bowel, stomach). However, the limited physical half-life of  $^{11}\text{C}$  (20 min) restricts its application to PET centers equipped with on-site cyclotron [22,23]. In response to this limitation, the development of  $^{18}\text{F}$ -labeled choline analogs has emerged. These analogues faithfully replicate the metabolic processing of native choline and are commercially available as PET imaging agents. This technological advancement extends the scope of imaging capabilities to facilities lacking on-site cyclotron access, broadening the horizons for diagnostic applications in diverse clinical settings. The advent of  $^{18}\text{F}$ -labeled choline analogues represents a significant stride in making advanced PET imaging more accessible and adaptable to a wider range of medical environments [24,25].

### 2.2.4. Receptors-targeting tracers

The first somatostatin analog to obtain approval by the Food and Drug Administration (FDA) in 1994 for planar and Single Photon Emission Computed Tomography (SPECT) imaging of neuroendocrine neoplasms (NENs) was [ $^{111}\text{In}$ ]In-pentetreotide. Somatostatin analogues allow in vivo visualization of the expression of somatostatin receptors (SSTRs) [26]. However, [ $^{111}\text{In}$ ]In-pentetreotide has unfavorable dosimetry and lower diagnostic performance compared to [ $^{68}\text{Ga}$ ]DOTA peptides ([ $^{68}\text{Ga}$ ]Ga-DOTA-TOC, [ $^{68}\text{Ga}$ ]Ga-DOTA-NOC, [ $^{68}\text{Ga}$ ]Ga-DOTA-TATE). These limitations have been attributed primarily to suboptimal physical characteristics of the radiopharmaceutical, high physiological uptake in the liver (a frequent site of NET metastasis), lower spatial resolution of gamma cameras, and increased patient discomfort due to prolonged acquisition times for imaging [27,28]. Radiopharmaceuticals currently used for somatostatin receptor (SSTR) PET/CT imaging share a common structure,

including a positron-emitting isotope ( $^{68}\text{Ga}$ ), a chelator (DOTA), and the SSTR ligand (NOC, TOC, TATE). These tracers, [ $^{68}\text{Ga}$ ]Ga-DOTA-TOC, [ $^{68}\text{Ga}$ ]Ga-DOTA-NOC, and [ $^{68}\text{Ga}$ ]Ga-DOTA-TATE, show a variable affinity for SSTR subtypes [29]. Although  $^{68}\text{Ga}$  has a short half-life (68 min) and is unsuitable for dosimetry or therapeutic purposes, radiopeptides function as SSTR receptor agonists through receptor activation and internalization upon binding. Despite differences in affinity for the various SSTR subtypes, the clinical performance of these radiopharmaceuticals is considered clinically comparable, as they all bind with high affinity to SSTR-2, the subtype predominantly expressed in most NENs [28]. Since its initial introduction into clinical practice, SSTR PET/CT has shown numerous advantages over SPECT/CT imaging, including higher spatial resolution and more favorable liver/gut biodistribution. It currently represents the gold standard functional imaging modality for NENs, receiving approval from various guidelines [28]. [ $^{68}\text{Ga}$ ]Ga-DOTA-TOC, the pioneer SSTR PET ligand developed in 2001, first gained approval in Europe in 2016 [30]. Features SSTR affinity profile similar to octreotide, with a notable affinity for SSTR-2 and -5, although lower than [ $^{68}\text{Ga}$ ]Ga-DOTA-NOC [31]. [ $^{68}\text{Ga}$ ]Ga-DOTA-NOC has a high affinity for SSTR-2,3,5 while [ $^{68}\text{Ga}$ ]Ga-DOTA-TATE shows the highest affinity for SSTR-2, boasting a tumor-to-background ratio higher than [ $^{68}\text{Ga}$ ]Ga-DOTA-NOC. When labeled with  $^{177}\text{Lu}$  (or  $^{90}\text{Y}$ ), SSTR analogs can be used for NEN peptide receptor radionuclide therapy (PRRT), approved by the EMA in 2017 and the FDA in 2018 [32,33].

## 3. Molecular imaging techniques

Planar imaging in nuclear medicine represents a projection of the radioactivity distribution of gamma-emitting radiopharmaceuticals at a fixed angle (anterior, posterior, lateral, oblique) [34]. Single Photon Emission Computed Tomography with Computed Tomography (SPECT/CT) is a powerful hybrid imaging technique that combines the functional information of SPECT with the anatomical details provided by CT [35]. Acquiring both SPECT and CT images simultaneously allows correction for nuclear image attenuation and anatomical localization of radiotracer uptake. To mitigate radiation exposure, the recommendation is to use low-dose CT, which results in relatively lower radiation doses (e.g. 1 mSv) and is considered sufficient when the aim of hybrid imaging is attenuation correction and anatomical referencing of SPECT lesions [36]. The addition of SPECT/CT to planar imaging, for example in [ $^{99\text{m}}\text{Tc}$ ]Tc-MIBI imaging, has become a valuable tool for parathyroid localization in primary hyperparathyroidism. It improves anatomical localization and allows correlation to anatomical findings in the CT image [37]. Commonly used SPECT radionuclides are listed in Table 1.

PET/CT is a valuable tool for visualizing molecular processes within the human body by utilizing specific positron-emitting radionuclides that interact with molecular pathways (Table 2).

**Table 1.** Gamma camera radionuclides.

Radionuclide	Half Life	Production	Energy
$^{99\text{m}}\text{Tc}$	6.02 hours	Generator	140 keV (89%)
$^{123}\text{I}$	13.22 hours	Cyclotron	159 keV (83%)
$^{131}\text{I}$	8.02 days	Nuclear reactor	364 keV (81%)

**Table 2.** positron emission tomography radionuclides.

Radionuclide	Half Life	Production	Positron energy (Max/mean)	Positron range (Mean/Max)
$^{18}\text{F}$	109.8 min	Cyclotron	0.65/0.28 MeV	2.5/0.7 mm
$^{68}\text{Ga}$	67.7 min	Generator	1.90/0.84 MeV	9.0/2.9 mm
$^{11}\text{C}$	20.04 min	Cyclotron	0.96/0.39 MeV	4.2/1.2 mm
$^{124}\text{I}$	4.2 days	Cyclotron	2.14/1.53 MeV	3.0/1.0 mm

The principle of coincidence detection in PET scanners involves capturing annihilation photons on opposite sides of a detector system. Low-dose CT improves anatomical localization, enhancing precision in identifying pathophysiological processes. The correlation between radionuclide accumulation intensity from PET and morphological changes revealed by CT aids in evaluating pathological conditions. Additionally, low-dose CT is essential for correcting photon attenuation by tissue, making it an indispensable tool in PET imaging [38]. Over the years, the development of PET scanners, with the introduction of digital PET, has led to improved image resolution and reduced radiation exposure due to reduced injected activity. The continuous table motion mode has emerged as an alternative acquisition mode, offering greater uniformity and sensitivity [39].

Positron Emission Tomography/Magnetic Resonance Imaging (PET/MRI) combines the strengths of PET and MRI in a single examination. Specifically, MRI provides detailed anatomical images with excellent soft tissue contrast and allows a reduction of radiation dose compared to PET/CT. However, its use is limited by high costs, reduced availability, and no substantial advantages over PET/CT in most oncological indications.

## 4. Thyroid: clinical applications

### 4.1. Hyperthyroidism

Thyrotoxicosis is a general term and refers to the clinical syndrome of excess circulating thyroid hormones and it's mostly caused by an increased thyroid hormone biosynthesis and secretion from the thyroid gland. Other causes of thyrotoxicosis are mainly represented by destructive thyroiditis where thyroid hormones are passively released by damaged follicular thyroid cells [40]. Depending by causes, intensity, and duration of thyrotoxicosis the clinical

presentation ranges from asymptomatic to life-threatening thyroid storm. Serum TSH measurement is pivotal to confirm (TSH <0.1 mUI/L) or rule-out (TSH >0.4 mUI/L) thyrotoxicosis, with values ranging between 0.1 and 0.4 mUI/L demanding a simple surveillance. Serum concentrations of free T4 and free T3 are useful to differentiate subclinical from overt thyrotoxicosis and assess the severity of the latter. The most frequent cause of thyrotoxicosis is due to diffuse (i.e. Graves disease, GD) or regional (i.e. uni- or multifocal AFTNs) thyroid hyperfunction (i.e. hyperthyroidism '*strictu sensu*') [41]. Particularly, 80–90% of hyperthyroid patients carry GD while <10% to 20% of patients carry AFTNs, the latter being more frequent in countries with current or previous iodine deficiency [2]. The remaining causes of thyrotoxicosis include destructive thyroiditis and iodine-induced and drug-induced dysfunction [40,42]. TSH receptor antibody (TRAb) measurement, TS or RAIU, and the US with color flow Doppler evaluation can be adopted to differentiate causes of thyrotoxicosis depending on their availability and preferences of attending physicians [43]. A study involving 124 patients with thyrotoxicosis compared TS, US, and two TRAb assays, respectively [44]. However, depending on locally available facilities, TRAb assays can be adopted as a first-line diagnostic option limiting the use of TS to TRAb-negative patients [40]. Finally, exogenous iodine overload must be always investigated in thyrotoxic patients as it may lead to a thyrotoxicosis with decreased uptake (i.e. expanded iodine pool) mimicking the early phase of destructive thyroiditis on TS [Figure 1] [43].

### 4.2. Non-toxic thyroid nodules

Thyroid nodules are frequently detected in daily-life clinical practice, and the attending physician is required to decide,

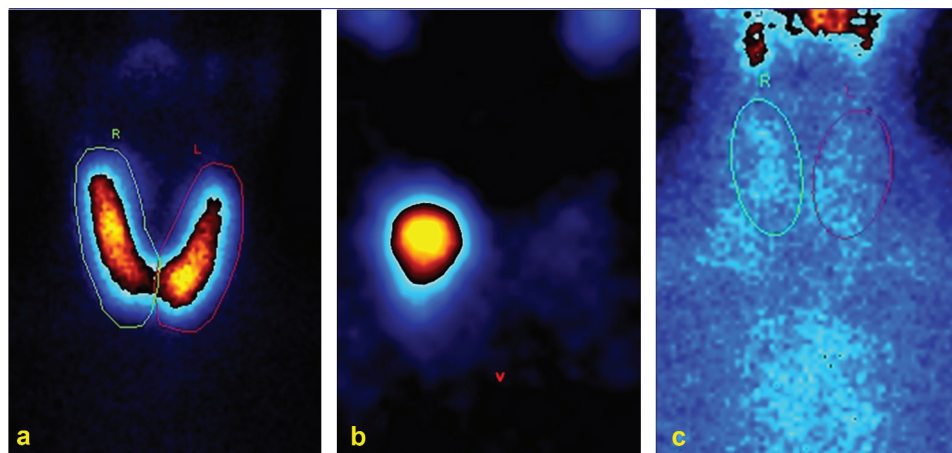


**Figure 1.**  $^{99\text{m}}\text{Tc}$ -pertechnetate scan presentation of Graves' disease (a), autonomously functioning thyroid nodules (b) and destructive thyroiditis (c).

which ones carry a significant risk of malignancy and address them to further workup with FNAC. Thyroid US accurately assesses morphologic and structural features, which have been recently adopted to derive a standardized risk assessment for thyroid malignancy under the different Thyroid Imaging And Data Reporting Systems (TI-RADS) in order to reduce the significant inter-operator variability [45–48]. Different TI-RADS systems combine, with some differences US features (i.e. shape, margins, echogenicity, composition, microcalcifications) in hierarchically tiered risk categories and, overall, demonstrated a satisfactory performance, especially in ruling-out nodules from FNAC. However, TI-RADS classifications inappropriately prompt FNAC in 27% to 90% of AFTNs depending on different adopted TI-RADS. While AFTNs have a 96%–99% negative predictive value (NPV) for malignancy, indeterminate cytologic features are frequently reported in such nodules, and FNAC procedures are discouraged in such cases [49,50]. As up to 50% and more AFTNs present with normal TSH in countries with inadequate iodine supply. The integration of regional iodine intake, local TSH reference range, size, and echostructure of the nodule may better inform the decision to perform TS in such cases [51]. Conversely, non-autonomous nodules can be managed using TI-RADS to select high-risk ones for FNAC and cytopathology assessment and avoid it in other cases. Thyroid cytopathology is generally reported using the standardized Bethesda system, which is accurate in detecting or excluding malignancy in most cases [52]. However, up to 25% of nodules fall in indeterminate categories (follicular lesion of undetermined significance or atypia of undetermined significance, Bethesda III; follicular neoplasm, Bethesda IV) with an attached risk of malignancy of 10%–50%. Therefore, diagnostic lobectomies or even thyroidectomies are still common in such cases with most nodules demonstrated to be benign on definitive histopathology. Currently, molecular biomarkers testing on FNAC material and molecular bioimaging with  $^{99m}\text{Tc}$ -MIBI and  $^{18}\text{F}$ FDG should be performed before diagnostic surgery [49]. A detailed analysis of molecular FNAC biomarkers is out of the scope of our present review and the reader is addressed to a recent extensive review [53].  $^{99m}\text{Tc}$ -MIBI thyroid scintigraphy has been used by several authors for more than 30 years in patients affected by hypofunctioning thyroid nodules with indeterminate cytology in order to better stratify the risk of having malignancy. Notably,

this method should not be used in patients with AFTNs as the increased metabolic activity of such nodule(s) is reflected by increased  $^{99m}\text{Tc}$ -MIBI uptake [54].

Hurtado-Lopez and colleagues first proposed a visual comparison of intranodular  $^{99m}\text{Tc}$ -MIBI and  $\text{Na}^{99m}\text{Tc}\text{TcO}_4$  uptake showing quite absolute negative predictive values (i.e. rule out test) [Figure 2] [55]. More recently, Campenni and colleagues proposed a semi-qualitative analysis comparing  $^{99m}\text{Tc}$ -MIBI uptake within the nodule and extra-nodular tissue, respectively, increasing the NPV up to 99% [56,57]. Notably, the accuracy is reduced in oxyphilic nodules (i.e. Hurthle cells adenoma) being these lesions rich in mitochondria: accordingly the use of  $^{99m}\text{Tc}$ -MIBI scintigraphy is discouraged in such setting [57,58].

$^{18}\text{F}$ FDG PET/CT is an established tool in many oncological diseases also including thyroid cancers [59]. In addition, its use has been proposed to support the differential diagnosis of benign vs malignant cytologically indeterminate thyroid nodules [Figure 3] [60]. Indeed, a  $^{18}\text{F}$ FDG-negative cytologically indeterminate nodule carries a negligible risk to be a malignant lesion (prevalence of malignancy < 5%) thus making  $^{18}\text{F}$ FDG PET/CT an accurate ruling-out test able to change the clinical management of such patients reducing inappropriate surgical procedures by 40% [60–63]. Conversely,  $^{18}\text{F}$ FDG PET/CT specificity is suboptimal as 50% of patients with a visually  $^{18}\text{F}$ FDG-positive pattern turn out of having a benign lesion at final histological report [49,60–62]. Radiomics analysis has been recently proposed in order to increase specificity and PPV of  $^{18}\text{F}$ FDG PET/CT (i.e. ruling-in test) in distinguishing benign from malignant cytologically indeterminate nodules [64]. However, up to date, available literature data showed contrasting results and radiomics cannot be proposed in daily clinical routine [49,65]. Finally, as  $^{99m}\text{Tc}$ -MIBI scintigraphy,  $^{18}\text{F}$ FDG PET/CT should not be performed in patients with Hurthle cell nodules since a high uptake is expected even in benign lesion [49,63].

#### 4.3. Follicular cells-derived thyroid cancers

Molecular imaging assumes an important role in the management of different thyroid cancers. In particular, imaging with iodine radioisotopes (i.e.  $^{131}\text{I}$ ,  $^{123}\text{I}$ ,  $^{124}\text{I}$ ) is pivotal in patients with DTC while  $^{18}\text{F}$ FDG PET/CT is useful to evaluate aggressive and RAI-R DTC [66].

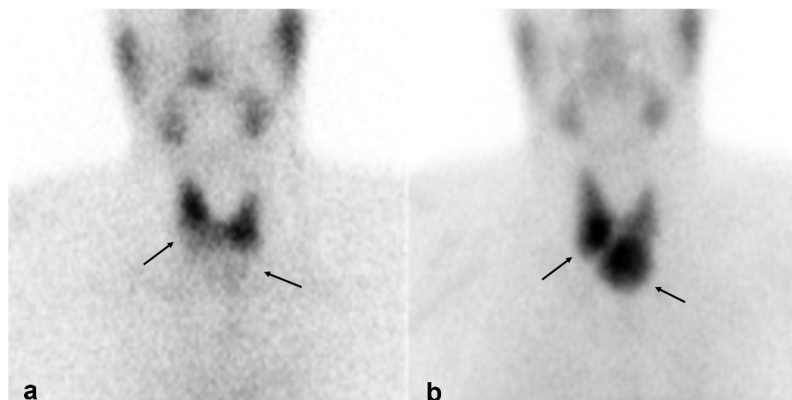


**Figure 2.**  $^{99m}\text{Tc}$ -pertechnetate (a) and  $^{99m}\text{Tc}$ -MIBI (b) scans: cold and MIBI active nodules in both lobes (arrows). Histopathology: multifocal invasive follicular variant of papillary thyroid carcinoma.

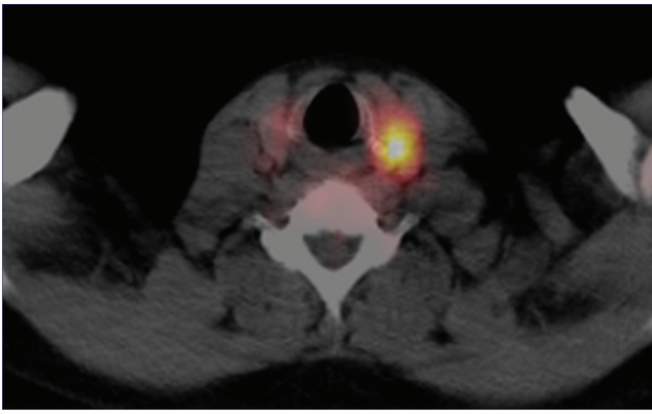


**Figure 3.**  $^{18}\text{F}$ FDG PET/CT (axial image): FDG-avid thyroid nodule (i.e. risk of malignancy about 30%).

#### 4.3.1. Post-therapy whole-body scintigraphy

A post-therapy whole body scintigraphy (pT-WBS) is always obtained 3–10 days after radioiodine therapy (RIT) in DTC patients [66–68]. It shows the location and extent of iodine-avid tissue and allows a more accurate staging by detecting unknown disease foci, refining the initial risk stratification, and tailoring additional therapies and follow-up strategies [66]. Whenever possible a pT-WBS should be completed with

a SPECT/CT in order to significantly increase its diagnostic accuracy [Figure 4] [66,69–71].

Notably, the therapeutic activity should be administered in a few days if a postoperative scan is performed (see below). In practice, however, this method is not practical considering the decision change in planned activities is not usually possible especially when radioiodine is ordered in capsule form.

#### 4.3.2. $^{123/131}\text{I}$ -postoperative diagnostic whole-body scintigraphy

Postoperative diagnostic whole-body scintigraphy (pDx-WBS) can be used as an additional diagnostic tool, in association with neck US and basal Tg measurement, for a more correct postoperative staging and risk stratification of DTC patients.

In lower-risk DTC patients in whom RIT is not indicated on a routine basis [72] a positive pDx-WBS may support RIT with a therapeutic schedule [73–76]. In higher-risk DTC patients (in whom RIT is already planned), pDx-WBS can serve as a guide for better choosing iodine-131 activity since it can detect and locate distant metastases [73,75,77] and modify the prescribed iodine-131 activity in up to 50% of cases [Figure 5] [78]. Finally, pDx-WBS can lead to alternative/additional therapies, especially in high-risk DTC patients with negative radioiodine imaging and positive  $^{18}\text{F}$ FDG PET/CT imaging [70,76,79].

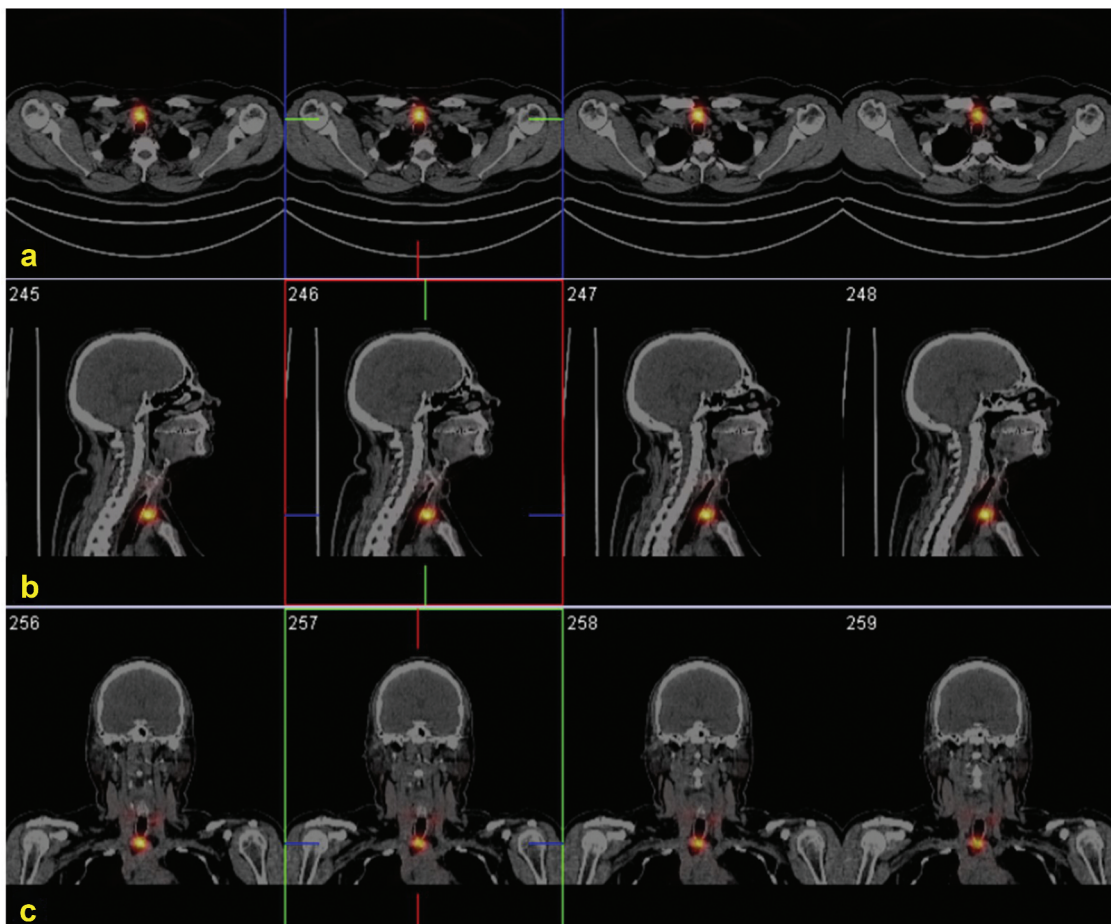


**Figure 4.** Post-ablation  $^{131}\text{I}$  SPECT/CT (B) in a young female affected by papillary thyroid carcinoma (pT2 Nx) showing a central neck lymph-node metastasis.

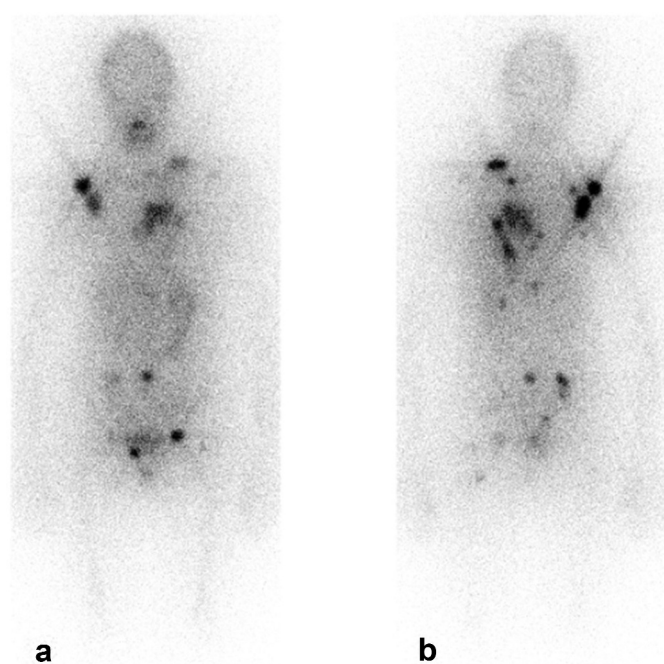


**Figure 5.** Post-therapy  $^{131}\text{I}$  WBS (a, anterior; b, posterior views) and SPECT/CT (C) in a 50 years old female affected by papillary thyroid carcinoma (pT2 N1b) showing multiple visceral and skeletal radioiodine-avid metastases.

#### 4.3.3. $^{123/131}\text{I}$ - diagnostic whole-body scintigraphy (Dx-WBS)

For many years Dx-WBS played an important role in the follow-up of DTC patients but in the last decades, its use has been progressively reduced since some authors argued about its low sensitivity and the induction of the so-called stunning effect related to the use of iodine-131 [72]. However, the diagnostic performance of Dx-WBS (is significantly improved by using hybrid imaging (i.e. SPECT/CT imaging) and performing the study according to basal Tg level while the so-called stunning effect can be avoided by using iodine-123 or administering the iodine-131 few days after diagnostic scanning, as already reported by robust literature data [74,75,80–82]. The use of  $^{123}\text{I}$ -Dx-WBS was recently proved to be able to detect incomplete structural response (mostly loco-regional) in patients with incomplete and indeterminate biochemical response at conventional restaging, especially in those patients with malignancies located in the isthmus [83,84].

#### 4.3.4. $^{124}\text{I}$ -positron emission tomography

The use of iodine-124, a radioisotope of iodine emitting positron (i.e.  $^{124}\text{I}$  PET/CT), may be considered as a potential alternative to iodine-123/131 being able to overtake by its favorable characteristics some intrinsic limits of 'conventional' iodine radioisotopes (i.e. iodine-123/131) such as the reduced spatial resolution of SPECT/CT. However, some concerns related to lower image quality compared to other positron emitters due to a complex decay scheme (interrupting gamma rays), no universally accepted imaging protocol or quantitation method, longer physical half-life compared to other PET agents, high cost (more expensive than other iodine radioisotopes) and low/ready availability must be considered

when its use in DTC patients is planned [73,85]. All in all, its use can be considered in (i) postoperative assessment of DTC, (ii) DTC patients with rising Tg/TgAb levels and negative nUS, (iii) informing lesion-based dosimetry in patients with advanced DTC taking advantage of improved spatial resolution of  $^{124}\text{I}$  PET/CT to quantify target volume, in vivo tumor concentration, and radionuclide biodistribution [85–91].

#### 4.3.5. $^{18}\text{F}$ FDG positron emission tomography

In DTC patients, the main indication for  $^{18}\text{F}$ FDG PET/CT is during follow-up when a persistent/recurrent disease is suspected due to high or increasing Tg levels (or TgAb as a surrogate marker), but nUS is negative or doubtful and Dx-WBS and/or pT-WBS are negative as well [66,73]. In this setting of patients, the use of  $^{18}\text{F}$ FDG PET/CT is supported by robust literature data in which pooled sensitivity and specificity ranging from 80% to 88% and from 84% to 90%, respectively, were reported [66,92–94]. However, it is important to take into account  $^{18}\text{F}$ FDG PET/CT sensitivity may be influenced by several factors such as the degree of de-differentiation, tumor burden, and, with more limited evidence, serum TSH level [73]. Regarding the optimal strategy to obtain  $^{18}\text{F}$ FDG PET/CT (i.e. basal  $^{18}\text{F}$ FDG PET/CT vs rhTSH-stimulated  $^{18}\text{F}$ FDG PET/CT), Leboulleux and colleagues in their prospective study found that the per-patient sensitivity was not different between basal and rhTSH-stimulated imaging studies. Conversely, the per-lesion sensitivity (i.e. the number of detected lesions) was higher using rhTSH-stimulation but this result changed the treatment plan in 6% of patients only [66,95]. According to 2015 ATA guidelines,  $^{18}\text{F}$ FDG PET/CT should be performed when stimulated Tg levels are  $>10$  ng/mL [72]. Giovanella and colleagues suggested performing  $^{18}\text{F}$ FDG PET/CT in DTC patients having a basal Tg level  $\geq 5.5$  ng/ml or in those in whom Tg doubling time is less than 1 year, regardless of the basal Tg value [96]. Finally,  $^{18}\text{F}$ FDG PET/CT assumes an important prognostic role in metastatic DTC patients representing high  $^{18}\text{F}$ FDG uptake as an independent and negative prognostic factor for overall survival and for disease-specific survival. In addition, a larger number of  $^{18}\text{F}$ FDG-avid metastatic lesions and a higher SUVmax are associated with a poor prognosis of patients [Figure 6] [97–99].

#### 4.4. Medullary thyroid carcinoma

Medullary thyroid carcinoma is frequently presented as a metastatic disease unless detected in early stages. Although patients with limited disease respond well to surgery, more than 50% of patients have lymph node or distant metastases and their detection is critical for the success of subsequent management. Following initial surgery, patients are carefully followed-up since patients with residual lymph node metastases after thyroidectomy are likely to benefit from re-operation. In clinical routine 2 to 3 months after initial surgery, CT and CEA measurement, and neck US are performed as a post-operative work-up [66]. Patients whose post-operative serum CT level is normal are considered 'biochemically cured' and have a 10-year survival rate of 97.7%. According to current clinical guidelines, clinical examination and neck US are required in patients with serum CT levels  $<150$  pg/mL, as such cases with recurrent disease usually have cervical lymph



**Figure 6.**  $^{18}\text{F}$ -FDG PET maximum intensity projection image of a patient with poorly differentiated thyroid carcinoma showing increasing radiopharmaceutical uptake within the thyroid, corresponding to the primary tumor site and multiple lymph node, lung, liver, bone and renal metastases.

node metastases [100]. Neck US, CT, MRI, and bone scintigraphy were traditionally recommended in patients with post-operative CT >150 pg/mL and/or increased CEA and/or shortened Ctn/CEA doubling time. However, additional PET/CT imaging should be considered when serum CT levels exceed 150 pg/mL, or the CT doubling time is shortened (i.e. <24 months), and conventional imaging results are inconclusive. Briefly,  $^{18}\text{F}$ FDOPA PET/CT is the radiotracer of choice due to its superior diagnostic performance compared with other PET tracers, especially when done with contrast-enhanced CT.  $^{18}\text{F}$ FDG PET/CT should be performed, in particular, if CT and CEA levels are rapidly rising (i.e. doubling time <1 year) or aggressive behavior of the disease is expected (e.g. CEA levels disproportionately higher than CT levels).  $^{68}\text{Ga}$ Ga SSA PET/CT could be considered in selected cases with inconclusive anatomic and  $^{18}\text{F}$ FDOPA/ $^{18}\text{F}$ FDG PET/CT imaging. Moreover,  $^{68}\text{Ga}$ Ga SSA PET/CT could assess the feasibility of peptide receptor radionuclide therapy in highly selected patients considered for this targeted treatment [101].

## 5. Primary hyperparathyroidism

Primary hyperparathyroidism is the third most common endocrine disorder caused by hyperfunctioning parathyroid gland(s) which are producing increased amounts of parathyroid hormone (PTH) [102]. It occurs up to 3× more commonly in females, especially in postmenopausal age [103,104]. Serum PTH concentration is increased, or within higher reference range but in combination with hypercalcemia. Conversely, normal serum calcium levels with an increased PTH occurs rarely, in so-called normocalcemic hyperparathyroidism [105]. Hyperfunctioning parathyroids are single adenomas in majority of patients (85%), while in approximately 15% of cases there is multiglandular disease (MGD) [106], in the form of multiple adenomas or hyperplasia, while parathyroid carcinoma is extremely rare. Parathyroid glands are typically located next to both thyroid lobes in 84% of cases, while ectopic glands occur in approximately 16% of cases [107]. Most individuals have four parathyroid glands, supernumerary glands (up to 8 of them) occur in up to 13% of cases [108,109], while in < 3% of cases, there are only 3 glands [108]. The most primary hyperparathyroidism (pHPT) cases are sporadic, while 5% are part of hereditary syndromes, e.g. multiple endocrine neoplasia types 1, 2, and 4 (MEN-1, MEN-2, and MEN-4) [110]. The only curative therapy is the parathyroidectomy of affected gland(s) [111]. Surgery is important not only in symptomatic, but also in asymptomatic patients as long-term hypercalcemia may affect many organs during the years [112]. Preoperative localization of the hyperfunctioning gland(s) allows more focused surgical approach e.g. minimally invasive parathyroidectomy (MIP) which reduces duration of the surgery, perioperative complications and morbidity, results in more favorable cosmetic outcome and patient contentment and has similar cure rates as bilateral neck exploration [111,113–116]. Radionuclide parathyroid imaging detects typically located glands, as well as ectopic. Sensitivity is generally greater in the case of adenomas compared to hyperplasia as in the latter case glands are usually smaller [117]. It is crucial to identify MGD, due to its impact on surgical procedure and therefore patient outcome. The second surgery is usually more challenging compared to the first one.

### 5.1. $^{99\text{m}}\text{Tc}$ ]Tc-MIBI imaging

The most widely used preoperative imaging strategy is the combination of  $^{99\text{m}}\text{Tc}$ ]Tc-MIBI SPECT/CT and cervical ultrasonography (cUS) [Figure 7] with a sensitivity from 80 to up to 95% mainly due to high sensitivity of  $^{99\text{m}}\text{Tc}$ ]Tc-MIBI scintigraphy [118]. In equivocal situations, cUS may be combined with targeted FNAC and measurement of PTH in the aspirate (FNAC-PTH) to increase the specificity for detection of hyperfunctioning parathyroid tissue in cUS-accessible regions in the neck [119].  $^{99\text{m}}\text{Tc}$ ]Tc-MIBI SPECT/(CT) demonstrates patient-based and lesion-based detection rate of 88% [120]. However, its sensitivity is much lower in patients with MGD (27–61%) compared to those with a single gland disease (80–92%) [121,122], a similar issue as with other imaging modalities. Parathyroid gland scintigraphy may be performed as dual-phase and dual-tracer method [Figure 8]. Dual-tracer scintigraphy with subtraction imaging has a higher

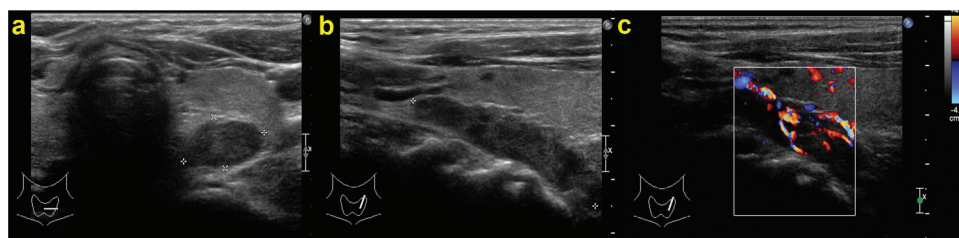


**Figure 7.** Parathyroid ultrasound: ovoidal hypoechoic nodule with vascular basket-pole, consistent with enlarged and hyperfunctioning parathyroid gland.

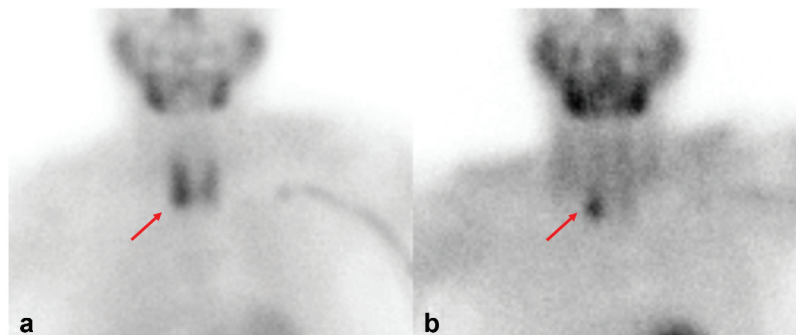


**Figure 8.**  $^{99m}\text{Tc}$ -MIBI dual phase scintigraphy: tracer uptake and late retention in a parathyroid adenoma (red arrow).

performance compared to dual-phase imaging, with sensitivity up to 95% [123,124]. SPECT images have higher sensitivity compared to planar images, while SPECT/CT provides anatomic correlation and localization of gland(s) [Figure 9]. False-positive imaging results may occasionally occur due to thyroiditis (in a single-tracer protocol), neck lymphadenopathy, and malignant or benign thyroid nodules [125]. False-negative results most commonly occur due to multiglandular disease, parathyroid hyperplasia and generally small-size parathyroid glands [125], and due to a small amount of oxyphil cells [32,33]. Our readers are referred to the *The EANM practice guidelines for parathyroid imaging* for details on imaging protocols and administered activities [118].

### 5.2. [ $^{99m}\text{Tc}$ ]Tc-tetrofosmin

[ $^{99m}\text{Tc}$ ]Tc-tetrofosmin is another SPECT tracer that is mainly used in a dual-tracer method in combination with thyroid gland

tracers Na[ $^{99m}\text{Tc}$ ]TcO<sub>4</sub> or Na[ $^{123}\text{I}$ ], as it doesn't show any thyroid wash-out. However, its use is limited, despite similar diagnostic performance to [ $^{99m}\text{Tc}$ ]Tc-MIBI [126–128].

### 5.3. [ $^{18}\text{F}$ ]fluorocholine and [ $^{11}\text{C}$ ]choline

The alternative first-line imaging procedure with higher sensitivity compared to [ $^{99m}\text{Tc}$ ]Tc-MIBI SPECT/CT is [ $^{18}\text{F}$ ]fluorocholine ([ $^{18}\text{F}$ ]FCH) PET/CT, very accurate even in cases with negative or inconclusive standard imaging methods, in pHTP cases as well as in sHPT, owing to a higher spatial resolution of PET technique [129]. A meta-analysis of 14 choline studies (12  $^{18}\text{F}$ - and 2  $^{11}\text{C}$ -labeled choline) reported pooled sensitivity and [Figure 10] PPV of choline tracers of 95% and 97%, respectively, in per-patient analysis, while in a per-lesion analysis, the same values were 92% and 92%, respectively [130]. Furthermore, a recent meta-analysis that included 22 studies demonstrated even higher sensitivity of [ $^{18}\text{F}$ ]FCH PET/CT of 97% [131]. In a sub-analysis where both [ $^{99m}\text{Tc}$ ]Tc-

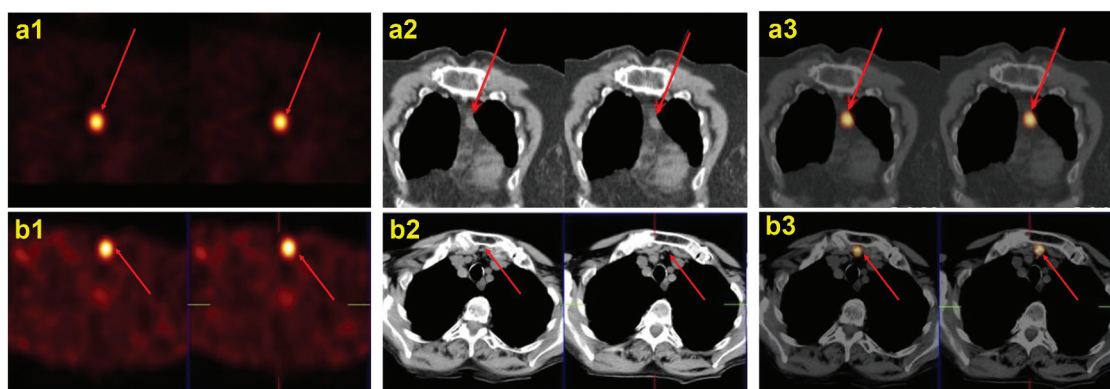


**Figure 9.**  $^{99m}\text{Tc}$ -MIBI SPECT/CT (coronal a-c, axial d-f): ectopic mediastinal parathyroid adenoma (red arrows).

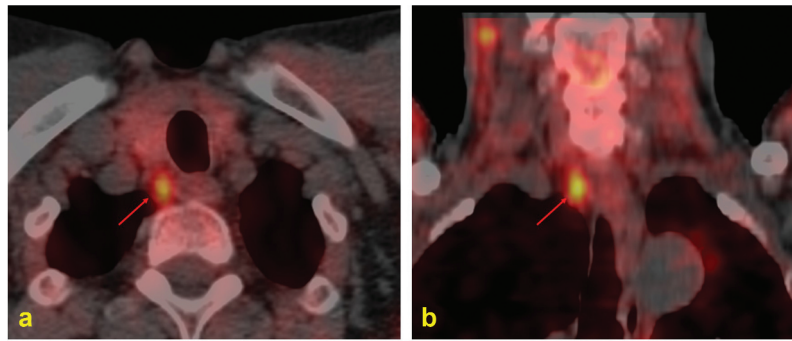


**Figure 10.**  $^{18}\text{F}$ -fluorocholine PET/CT (axial a, coronal b): parathyroid adenoma (red arrows).

MIBI and  $^{18}\text{F}$ ]FCH were included,  $^{18}\text{F}$ ]FCH also had a significantly higher sensitivity (96%) compared to  $^{99\text{m}}\text{Tc}$ ]Tc-MIBI (54%). Therefore,  $^{18}\text{F}$ ]FCH PET/CT is considered as a 'one-stop-shop' method for the detection of hyperfunctioning parathyroid glands [132]. It is important to emphasize that digital scanners have higher performance compared to analog scanners [133]. Parathyroid glands detected exclusively by the digital PET/CT are usually smaller than 10 mm, underlining the importance of these scanners in localizing small glands, which are usually associated with parathyroid gland hyperplasia. Other advantages of  $^{18}\text{F}$ ]FCH PET/CT, compared to conventional scintigraphic methods are lower radiation burden, improved resolution, and shorter acquisition time [118]. Potential limitations are the uptake by thyroid nodules and inflammatory lymph nodes as a potential cause of false-positive results [134] (also noticed in the case of other tracers), and reimbursement and licensing issues. Although  $^{18}\text{F}$ ]FCH PET/CT is more expensive compared to conventional scintigraphic methods, complete data on cost-effectiveness are needed as patients often require additional second-line imaging in case of negative or inconclusive first-line scintigraphic imaging methods.  $^{18}\text{F}$ ]FCH PET may be combined with 4D-CT and according to current data seems to be superior than  $^{18}\text{F}$ ]FCH PET or 4D-CT alone [135].  $^{18}\text{F}$ ]FCH is also used in PET/MRI systems. This method is very promising in a first- and second-line imaging setting, due to excellent diagnostic performance owing to the higher tissue contrast of MRI and significantly lower radiation exposure compared to scintigraphic methods and  $^{18}\text{F}$ ]FCH PET/CT [136–139]. It is particularly useful in hyperfunctioning glands with low  $^{18}\text{F}$ ]FCH uptake [140].

$^{11}\text{C}$ ]choline ( $^{11}\text{C}$ ]CH) accumulates in the parathyroid glands with the same mechanism as its analogue  $^{18}\text{F}$ ]FCH, and has very similar diagnostic performance [141,142]. The advantage of  $^{11}\text{C}$ ]CH PET imaging compared to scintigraphic methods and  $^{18}\text{F}$ ]FCH PET/CT is acquisition within 30 min from injection and significantly lower radiation exposure, owing to the short physical half-life of  $^{11}\text{C}$ . However, due to its short half-life, the use of  $^{11}\text{C}$ ]CH is limited to institutions with an on-site cyclotron. Furthermore,  $^{11}\text{C}$  has a higher average positron energy compared to  $^{18}\text{F}$  which results in more noise in the images and lower spatial resolution compared to  $^{18}\text{F}$ ]FCH images.

#### 5.4. $^{11}\text{C}$ ]methionine

$^{11}\text{C}$ ]MET is a second-line imaging PET tracer used after negative or inconclusive first-line imaging. It is accumulated in the

hyperfunctioning parathyroid glands presumably due to involvement in the process of PTH precursor synthesis [143]. A meta-analysis of 14  $^{11}\text{C}$ ]MET studies demonstrated its pooled sensitivity and pooled PPV of 77% and 98%, respectively, for the correct localization of hyperfunctioning parathyroid gland(s) [144]. Interestingly, there was no statistically significant difference in the sensitivity between patients without specific selection compared to those with negative or discordant standard imaging. A recent meta-analysis that compared the diagnostic performance of  $^{18}\text{F}$ ]FCH PET/CT with  $^{11}\text{C}$ ]MET PET/CT in patients with pHPT, revealed higher pooled sensitivity of  $^{18}\text{F}$ ]FCH PET/CT compared to  $^{11}\text{C}$ ]MET PET (92% vs. 80%, respectively), while the PPV values were similarly high (94% vs. 95%, respectively) [145].

The major limitations of this tracer are a very short physical half-life of  $^{11}\text{C}$  which limits its use to institutions with an on-site cyclotron, a relatively higher average positron energy of  $^{11}\text{C}$  compared to  $^{18}\text{F}$  resulting in images with more noise, and local reimbursement and licensing issues. Furthermore, thyroid nodules may also have high  $^{11}\text{C}$ ]MET uptake and cause false-positive results [106,107].

## 6. Parathyroid cancer

Parathyroid cancer is marked with high hypercalcemia and very high PTH levels. However, there are no specific biochemical data that may differentiate it from parathyroid adenoma or hyperplasia. Parathyroid cancer and its metastases usually accumulate  $^{99\text{m}}\text{Tc}$ ]Tc-MIBI [146–151], and have its higher retention compared to benign hyperfunctioning glands [152].  $^{18}\text{F}$ ]FCH also shows uptake in parathyroid cancer and its metastases [149,153,154].  $^{18}\text{F}$ ]FDG PET/CT is useful in detection of loco-regional and distant metastases, presumably in less differentiated lesions [147,155]. CT and MRI may also be useful for the evaluation of the local and distant spreading. Fine-needle aspiration cytology is not recommended because it is not accurate in diagnosing parathyroid carcinoma, and, most importantly, it may cause seeding of parathyroid cancer [156]. Finally, promising results were recently obtained with  $^{68}\text{Ga}$ ]Ga SSA PET/CT [158].

## 7. Conclusion

In the last years, improvements in molecular imaging modalities allowed a more reliable management of benign and malignant

thyroid and parathyroid diseases. Particularly, thyroid scintigraphy remains integral in detecting AFTNs and ruling out malignancy in cytologically indeterminate nodules. Moreover, a whole-body scan with SPECT/CT is pivotal after administration of therapeutic radioiodine activities in order to refine the clinical staging and assess the iodine-avidity of tumor lesions. PET/CT with [ $^{18}\text{F}$ ]FDG proved to be useful in excluding malignancy in cytologically indeterminate nodules as a suitable alternative to [ $^{99\text{m}}\text{Tc}$ ]Tc-MIBI. Moreover, [ $^{18}\text{F}$ ]FDG PET/CT is a useful complement imaging in DTC patients with increasing Tg levels and negative radioiodine whole-body scan and is a first-line procedure to stage and restage patients with RAI-R DTC and aggressive thyroid cancers. Among MTC patients PET/CT with [ $^{18}\text{F}$ ]FDOPA is the preferred molecular imaging procedure to restage patients with increasing biomarkers (CT, CEA) after surgery while [ $^{18}\text{F}$ ]FDG imaging proved to be useful in aggressive MTC (shortened CT and CEA doubling time, increased CEA > CT). Scintigraphic and SPECT/CT imaging with [ $^{99\text{m}}\text{Tc}$ ]Tc-MIBI, combined with cUS, is widely available and accurate in localizing hyperfunctioning parathyroid glands before surgery. However, [ $^{18}\text{F}$ ]FCH PET/CT gained momentum by providing the highest accuracy and is now proposed as a first-line one-shot imaging technique in patients with hyperparathyroidism.

## 8. Expert opinion

For decades molecular imaging and nuclear medicine methods allowed metabolic, functional and molecular characterization of the thyroid gland and informed clinical decisions (i.e. tailored radioiodine therapy for hyperthyroidism and DTC, respectively). Even if accurate non-radioisotopic methods emerged over time, the selective and optimized use of thyroid scintigraphy remains integral in different clinical scenarios. As illustrated in the present review its contribution is well established in patients presenting with thyrotoxicosis (i.e. differential diagnosis between productive and destructive thyrotoxicosis, differential diagnosis between diffuse or focal thyroid hyperfunction) and thyroid nodules (i.e. detection of AFTN and characterization of cytologically indeterminate cold nodules, respectively). Whole body scintigraphy examination is mandatory in all DTC patients shortly (2–7 days) after therapeutic administration of radioiodine in order to evaluate the extent of thyroid remnants, detect or exclude metastasis and refine post-operative staging. The role of diagnostic WBS with low activities of iodine-131 or, alternatively, iodine-123 is either before radioiodine therapy or during long-term follow-up is debated but such methods can be adopted in selected cases to refine therapeutic indication and disease's restaging, respectively. In the last decade, the diffusion of SPECT/CT tomographs greatly ameliorated the diagnostic accuracy of planar scintigraphy and, especially, WBS allowing a more precise evaluation of the thyroid gland volume and location (i.e. intra-thoracic goiters) and an accurate differentiation between thyroid remnants and iodine-avid neck lymph nodes and a precise localization of distant metastasis in DTC patients. Iodine-124 and [ $^{18}\text{F}$ ]TFT are promising alternative to high-activity iodine-131 to image DTC before and after radioiodine therapy but their clinical application is still hampered by logistical problems and related costs. [ $^{18}\text{F}$ ]FDOPA is the preferred method in patients with relapsing MTC but new tracers are urgently needed as the availability of [ $^{18}\text{F}$ ]FDOPA is limited in many countries and the performance of available alternatives as [ $^{68}\text{Ga}$ ]Ga-somatostatin

analogues (SSA) is suboptimal. While FDG is not a specific tracer of either DTC and MTC cells, [ $^{18}\text{F}$ ]FDG PET/CT is recommended when serum Tg is increasing despite negative radioiodine imaging and to stage and restage aggressive and radioiodine-refractory cancers as well as in patients with aggressive MTC. Its use will likely increase with the introduction of new theranostic approaches for radioiodine-refractory (RAI-R) DTC and advanced MTC. In fact, a high FDG uptake is related to a lower response rate and, consequently, [ $^{18}\text{F}$ ]FDG PET/CT should be used as biomarker to refine patients' selection. Finally, PET/CT with [ $^{68}\text{Ga}$ ]Ga-somatostatin analogues (SSA) is increasingly employed to select patients with advanced DTC and MTC for therapy with [ $^{177}\text{Lu}$ ]Lu-SSA. Notably, the results of such approaches are still preliminary and, for the moment, this theranostic approach should be restricted (outside clinical trials) to selected cases after appropriate multidisciplinary discussion. Finally, the use of nuclear imaging methods is firmly established in patients with proven primary hyperparathyroidism in order to precisely localize the overactive parathyroid(s) and inform selective and mini-invasive surgery. [ $^{99\text{m}}\text{Tc}$ ]Tc-MIBI scintigraphy in combination with neck US in experienced hands is a first-line imaging strategy suggested in many guidelines. However, [ $^{18}\text{F}$ ]FCH-PET/CT has shown even better performance, particularly in cases of negative/inconclusive conventional imaging methods, and it is today considered an alternative first-line imaging method, i.e. 'one-stop-shop' technique. It has a higher resolution, lower radiation burden, allows for a shorter imaging procedure compared to [ $^{99\text{m}}\text{Tc}$ ]Tc-MIBI SPECT/CT and, in our opinion, will replace other imaging methods in the next future.

## Funding

This paper was not funded.

## Declaration of interest

The authors have no relevant affiliations or financial involvement with any organization or entity with a financial interest in or financial conflict with the subject matter or materials discussed in the manuscript. This includes employment, consultancies, honoraria, stock ownership or options, expert testimony, grants or patents received or pending, or royalties.

## Reviewer disclosures

Peer reviewers on this manuscript have no relevant financial or other relationships to disclose.

## ORCID

Luca Giovannella  <http://orcid.org/0000-0003-0230-0974>

## References

**Papers of special note have been highlighted as either of interest (•) or of considerable interest (••) to readers.**

1. Historical Timeline - SNMMI [Internet]. [cited 2024 Jan 27]. Available from: <https://www.snmmi.org/AboutSNMMI/Content.aspx?ItemNumber=4175>
2. Campenni A, Avram AM, Verburg FA, et al. The EANM guideline on radioiodine therapy of benign thyroid disease. *Eur J Nucl Med Mol Imaging*. 2023 [cited 2023 Oct 2];50:[Internet]. 11):3324–3348.

- Available from: <https://link.springer.com/article/10.1007/s00259-023-06274-5>
- **The new EANM guideline dedicated to radioiodine therapy of benign thyroid diseases, including the role of different imaging procedures.**
  3. Ravera S, Reyna-Neyra A, Ferrandino G, et al. The sodium/iodide symporter (nis): molecular physiology and preclinical and clinical applications. *Annu Rev Physiol* [Internet]. 2017 [cited 2024 Jan 27];79(1):261–289. Available from: <https://pubmed.ncbi.nlm.nih.gov/28192058/>
  4. Ramos CD, Zantut Wittmann DE, Sá De Camargo Etchebehere EC, et al. Thyroid uptake and scintigraphy using 99mTc pertechnetate: standardization in normal individuals. *Sao Paulo Med J* [Internet]. 2002 [cited 2024 Jan 27];120(2):45–48. Available from: <https://pubmed.ncbi.nlm.nih.gov/11994772/>
  5. Chung JK. Sodium iodide symporter: its role in nuclear medicine. *J Nucl Med* [Internet]. 2002 [cited 2024 Jan 27];43:1188–1200. Available from: <https://pubmed.ncbi.nlm.nih.gov/12215558/>
  6. Chiu ML, Kronauge JF, Piwnica-Worms D. Effect of mitochondrial and plasma membrane potentials on accumulation of hexakis (2-methoxyisobutylisonitrile) technetium(I) in cultured mouse fibroblasts. *J Nucl Med* [Internet]. 1990 [cited 2024 Jan 27];31:1646–1653. Available from: <https://pubmed.ncbi.nlm.nih.gov/2213187/>
  7. O'Doherty MJ, Kettle AG, Wells P, et al. Parathyroid imaging with technetium-99m-sestamibi: preoperative localization and tissue uptake studies. *J Nucl Med*. 1992;33(3):313–318.
  8. Piwnica-Worms D, Holman BL. Noncardiac applications of hexakis(alkylisonitrile) technetium-99m complexes [Internet]. *J Nucl Med*. 1990 [cited 2024 Jan 27];1166–1167. Available from: <https://pubmed.ncbi.nlm.nih.gov/2362196/>
  9. Coakley AJ, Kettle AG, Wells CP, et al. 99Tcm sestamibi — a new agent for parathyroid imaging. *Nuclear Medicine Communications* [Internet]. 1989 [cited 2019 Dec 9];10(11):791–794. Available from: <http://www.ncbi.nlm.nih.gov/pubmed/2532313>
  10. Földes I, Lévy A, Stotz G. Comparative scanning of thyroid nodules with technetium-99m pertechnetate and technetium-99m methoxyisobutylisonitrile. *Eur J Nucl Med* [Internet]. 1993 [cited 2024 Jan 27];20(4):330–333. Available from: <https://pubmed.ncbi.nlm.nih.gov/8387921/>
  11. Listewnik MH, Piwowarska-Bilska H, Safranow K, et al. The diagnostic value of dual-phase SPECT/CT scintigraphy based on transport kinetics of 99mTc-sestamibi confirmed with histopathological findings in patients with secondary hyperparathyroidism — practical consideration. *Nucl Med Rev Cent East Eur* [Internet]. 2020 [cited 2024 Jan 27];23(2):71–77. Available from: <https://pubmed.ncbi.nlm.nih.gov/33007093/>
  12. Sandrock D, Merino MJ, Norton JA, et al. Ultrastructural histology correlates with results of thallium-201/technetium-99m parathyroid subtraction scintigraphy. *J Nucl Med* [Internet]. 1993 [cited 2024 Jan 27];34:24–29. Available from: <https://pubmed.ncbi.nlm.nih.gov/8418265/>
  13. Becker J, Schwarzenböck SM, Krause BJ. FDG PET hybrid imaging. recent, Results Cancer Res [Internet]. 2020 [cited 2024 Jan 27];216:625–667. Available from: <https://pubmed.ncbi.nlm.nih.gov/32594401/>
  14. Nanni C. PET-FDG: Impetus. *Cancers (Basel)* [Internet]. 2020 [cited 2024 Jan 27];12. Available from 4):1030. Available from: <https://pubmed.ncbi.nlm.nih.gov/32331374/>
  15. Uehara M, Morita H. FDG-PET. *Int Heart J* [Internet]. 2023 [cited 2024 Jan 27];64(2):125–127. Available from: <https://pubmed.ncbi.nlm.nih.gov/37005309/>
  16. Chierichetti F, Pizzolato G. 18F-FDG-PET/CT. *Q J Nucl Med Mol Imaging* [Internet]. 2012 [cited 2024 Jan 27];56:138–150. Available from: <https://pubmed.ncbi.nlm.nih.gov/22617236/>
  17. Krause BJ, Schwarzenböck S, Souvatzoglou M. FDG PET and PET/CT. Recent Results Cancer Res [Internet]. 2013 [cited 2024 Jan 27];187:351–369. Available from: <https://pubmed.ncbi.nlm.nih.gov/23179888/>
  18. Kuker R, Szejnberg M, Gulec S. I-124 Imaging and Dosimetry. *Mol Imaging Radionucl Ther* [Internet]. 2017 [cited 2024 Jan 27];26(1- (1)):66–73. Available from: <https://pubmed.ncbi.nlm.nih.gov/28117290/>
  19. Jiang H, DeGrado TR. [18 F]Tetrafluoroborate ([18 F]TFB) and its analogs for PET imaging of the sodium/iodide symporter. *Theranostics* [Internet]. 2018 [cited 2021 Dec 2];8:3918–3931. Available from: <https://pubmed.ncbi.nlm.nih.gov/30083270/>
  20. Podo F. Tumour phospholipid metabolism. *NMR Biomed* [Internet]. 1999 [cited 2024 Jan 27];12(7):413–439. Available from: <https://pubmed.ncbi.nlm.nih.gov/10654290/>
  21. Hara T, Kosaka N, Kishi H. PET imaging of prostate cancer using carbon-11-choline. *J Nucl Med* [Internet]. 1998 [cited 2024 Jan 27];39:990–995. Available from: <https://pubmed.ncbi.nlm.nih.gov/9627331/>
  22. Broos WAM, Wondergem M, van der Zant FM, et al. Dual-Time-Point 18F-Fluorocholine PET/CT in Parathyroid Imaging. *J Nucl Med* [Internet]. 2019 [cited 2024 Jan 27];60(11):1605–1610. Available from: <https://pubmed.ncbi.nlm.nih.gov/30877179/>
  23. Orevi M, Freedman N, Mishani E, et al. Localization of parathyroid adenoma by <sup>11</sup>C-choline PET/CT: preliminary results. *Clin Nucl Med* [Internet]. 2014 [cited 2019 Nov 13];39(12):1033–1038. Available from: <http://www.ncbi.nlm.nih.gov/pubmed/25290292>
  24. Rizzo A, Racca M, Cauda S, et al. 18F-fluorocholine PET/CT semi-quantitative analysis in patients affected by primary hyperparathyroidism: a comparison between laboratory and functional data. *Endocrine* [Internet]. 2023 [cited 2024 Jan 27];80(2):433–440. Available from: <https://pubmed.ncbi.nlm.nih.gov/36495390/>
  25. Talbot JN, Périé S, Tassart M, et al. 18F-fluorocholine PET/CT detects parathyroid gland hyperplasia as well as adenoma: 401 PET/CTs in one center. *Q J Nucl Med Mol Imaging* [Internet]. 2023 [cited 2023 Nov 23];67(2):96–113. Available from: <https://pubmed.ncbi.nlm.nih.gov/36995286/>
  26. Gabriel M, Decristoforo C, Kendler D, et al. 68Ga-DOTA-Tyr3-octreotide PET in neuroendocrine tumors: comparison with somatostatin receptor scintigraphy and CT. *J Nucl Med* [Internet]. 2007 [cited 2024 Jan 27];48(4):508–518. Available from: <https://pubmed.ncbi.nlm.nih.gov/17401086/>
  27. Sundin A, Arnold R, Baudin E, et al. ENETS Consensus Guidelines for the Standards of Care in Neuroendocrine Tumors: Radiological, Nuclear Medicine & Hybrid Imaging. *Neuroendocrinology* [Internet]. 2017 [cited 2024 Jan 27];105(3):212–244. Available from: <https://pubmed.ncbi.nlm.nih.gov/28355596/>
  28. Kwekkeboom DJ, Krenning EP, Lebtahi R, et al. ENETS Consensus Guidelines for the Standards of Care in Neuroendocrine Tumors: peptide receptor radionuclide therapy with radiolabeled somatostatin analogs. *Neuroendocrinology* [Internet]. 2009 [cited 2024 Jan 27];90(2):220–226. Available from: <https://pubmed.ncbi.nlm.nih.gov/19713714/>
  29. Bushnell DL, Baum RP. Standard imaging techniques for neuroendocrine tumors. *Endocrinol Metab Clin North Am* [Internet]. 2011 [cited 2024 Jan 27];40(1):153–162. Available from: <https://pubmed.ncbi.nlm.nih.gov/21349416/>
  30. Henrich U, Benešová M. [68Ga]Ga-DOTA-TOC: The First FDA-Approved 68Ga-Radiopharmaceutical for PET Imaging. *Pharmaceuticals (Basel)* [Internet]. 2020 [cited 2024 Jan 27];13. Available from: <https://pubmed.ncbi.nlm.nih.gov/32138377/>
  31. Yu J, Cao F, Zhao X, et al. Correlation and Comparison of Somatostatin Receptor Type 2 Immunohistochemical Scoring Systems with 68Ga-DOTATATE Positron Emission Tomography/Computed Tomography Imaging in Gastroenteropancreatic Neuroendocrine Neoplasms. *Neuroendocrinology* [Internet]. 2022 [cited 2024 Jan 27];112:358–369. Available from: <https://pubmed.ncbi.nlm.nih.gov/34077939/>
  32. Hope TA, Bergsland EK, Bozkurt MF, et al. Appropriate Use Criteria for Somatostatin Receptor PET Imaging in Neuroendocrine Tumors. *J Nucl Med* [Internet]. 2018 [cited 2024 Jan 27];59(1):66–74. Available from: <https://pubmed.ncbi.nlm.nih.gov/29025982/>
  33. Bozkurt MF, Virgolini I, Balogova S, et al. Guideline for PET/CT imaging of neuroendocrine neoplasms with 68Ga-DOTA-conjugated

- somatostatin receptor targeting peptides and 18F-DOPA. *Eur J Nucl Med Mol Imaging* [Internet]. 2017 [cited 2020 Dec 1];44(9):1588–1601. Available from: <https://doi.org/10.1007/s00259-017-3728-y>
34. Zanzonico P. Principles of nuclear medicine imaging: planar, SPECT, PET, multi-modality, and autoradiography systems. *Radiat Res* [Internet]. 2012 [cited 2024 Jan 28];177(4):349–364. Available from: <https://pubmed.ncbi.nlm.nih.gov/22364319/>
  35. Ljungberg M, Pretorius PH. SPECT/CT: an update on technological developments and clinical applications. *Br J Radiol* [Internet]. 2018 [cited 2024 Jan 28];91. Available from 1081):20160402. Available from: <https://pubmed.ncbi.nlm.nih.gov/27845567/>
  36. Buck AK, Nekolla S, Ziegler S, et al. SPECT/CT. *J Nucl Med* [Internet]. 2008 [cited 2024 Jan 28];49(8):1305–1319. Available from: <https://pubmed.ncbi.nlm.nih.gov/18632825/>
  37. Mallick R, Malik J, Yip L, et al. Novel Findings on SPECT-CT Tc-99 Sestamibi Imaging for Primary Hyperparathyroidism. *J surg res* [Internet]. 2020 [cited 2024 Jan 28];252:216–221. Available from: <https://pubmed.ncbi.nlm.nih.gov/32289578/>
  38. Vaquero JJ, Kinahan P. Positron Emission Tomography: Current Challenges and Opportunities for Technological Advances in Clinical and Preclinical Imaging Systems. *Annu Rev Biomed Eng* [Internet]. 2015 [cited 2024 Jan 28];17(1):385–414. Available from: <https://pubmed.ncbi.nlm.nih.gov/26643024/>
  39. Rausch I, Cal-González J, Dapra D, et al. Performance evaluation of the Biograph mCT Flow PET/CT system according to the NEMA NU2-2012 standard. *EJNMMI Phys* [Internet]. 2015 [cited 2024 Jan 28];2(1):1–17. Available from: <https://pubmed.ncbi.nlm.nih.gov/26501827/>
  40. Petranović Ovčariček P, Gorges R, Giovanella L. Autoimmune Thyroid Diseases. *Semin Nucl Med* [Internet]. 2023 [cited 2023 Dec 30]. Available from: <https://pubmed.ncbi.nlm.nih.gov/38044176/>
  41. Giovanella L, Ovčariček P P. Functional and molecular thyroid imaging. *The quarterly journal of nuclear medicine and molecular imaging* [Internet]. *The Q J Nucl Med and Mol Imaging*. 2022 [cited 2024 Jan 6];66(2):86–92. Available from: <https://pubmed.ncbi.nlm.nih.gov/35166094/>
  42. Petranović Ovčariček P, Deandreis D, Giovanella L. Thyroid dysfunctions induced by molecular cancer therapies: a synopsis for nuclear medicine thyroidologists. *Eur J Nucl Med and Molecular Imaging* 2021 [Internet]. 2021 [cited 2021 Jul 19];1–6. Available from: <https://link.springer.com/article/10.1007/s00259-021-05394-0>
  43. Giovanella L, Avram AM, Ovčariček PP, et al. Thyroid functional and molecular imaging. *Presse Med* [Internet]. 2022 [cited 2024 Jan 6];51. Available from 2):104116. Available from: <https://pubmed.ncbi.nlm.nih.gov/35124101/>
  44. Scappaticcio L, Trimboli P, Keller F, et al. Diagnostic testing for graves' or non-graves' hyperthyroidism: a comparison of two thyrotropin receptor antibody immunoassays with thyroid scintigraphy and ultrasonography. *Clin Endocrinol (Oxf)*. 2020;92(2):169–178. doi: 10.1111/cen.14130
  45. Tessler FN, Middleton WD, Grant EG, et al. ACR Thyroid Imaging, Reporting and Data System (TI-RADS): White Paper of the ACR TI-RADS Committee. *J Am Coll Radiol* [Internet]. 2017 [cited 2023 Oct 25];14(5):587–595. Available from: <https://pubmed.ncbi.nlm.nih.gov/28372962/>
  46. Zhou JQ, Yin LX, Wei X, et al. 2020 Chinese guidelines for ultrasound malignancy risk stratification of thyroid nodules: the C-TIRADS. *Endocrine* [Internet]. 2020 [cited 2023 Oct 25];70(2):256–279. Available from: <https://pubmed.ncbi.nlm.nih.gov/32827126/>
  47. Russ G, Bonnema SJ, Erdogan MF, et al. European Thyroid Association Guidelines for Ultrasound Malignancy Risk Stratification of Thyroid Nodules in Adults: The EU-TIRADS. *Eur Thyroid J* [Internet]. 2017 [cited 2022 Aug 31];6(5):225–237. Available from: <https://pubmed.ncbi.nlm.nih.gov/29167761/>
  48. Seifert P, Schenke S, Zimny M, et al. Diagnostic Performance of Kwak, EU, ACR, and Korean TIRADS as Well as ATA Guidelines for the Ultrasound Risk Stratification of Non-Autonomously Functioning Thyroid Nodules in a Region with Long History of Iodine Deficiency: A German Multicenter Trial. *Cancers (Basel)* [Internet]. 2021 [cited 2023 Oct 25];13(17):4467. Available from: <https://pubmed.ncbi.nlm.nih.gov/34503277/>
  49. Giovanella L, Campenni A, Tuncel M, et al. Integrated Diagnostics of Thyroid Nodules. *Cancers (Basel)* [Internet]. 2024 [cited 2024 Feb 24];16. Available from 2):311. Available from: <https://pubmed.ncbi.nlm.nih.gov/38254799/>
  50. Schenke SA, Groener D, Grunert M, et al. Integrated Thyroid Imaging: Ultrasound and Scintigraphy. In: Giovanella L, editor. *Integrated Diagnostics and Theranostics of Thyroid Diseases* [Internet]. Cham: Springer; 2023 [cited 2023 Dec 21]. p. 25–62. Available from: [https://link.springer.com/chapter/10.1007/978-3-031-35213-3\\_4](https://link.springer.com/chapter/10.1007/978-3-031-35213-3_4)
  51. Kreissl MC, Ovčariček PP, Campenni A, et al. The European Association of Nuclear Medicine (EANM)'s Response to the 2023 European Thyroid Association (ETA) clinical practice guidelines for thyroid nodule management and nuclear medicine: a deliberate oversight?. *Eur J Nucl Med Mol Imaging* [Internet]. 2024 [cited 2024 Feb 25]. Available from: <https://pubmed.ncbi.nlm.nih.gov/38226985/>
  52. Ali SZ, Baloch ZW, Cochand-Priollet B, et al. The 2023 Bethesda System for Reporting Thyroid Cytopathology. *Thyroid* [Internet]. 2023 [cited 2023 Oct 21];33. Available from: <https://pubmed.ncbi.nlm.nih.gov/37427847/>
  53. Rossi ED, Locantore P, Bruno C, et al. Molecular Characterization of Thyroid Follicular Lesions in the Era of “Next-Generation” Techniques. *Front Endocrinol* [Internet]. 2022 [cited 2024 Feb 24];13. Available from: <https://pubmed.ncbi.nlm.nih.gov/35634500/>
  54. Giovanella L, Ceriani L, Treglia G. Role of isotope scan, including positron emission tomography/computed tomography, in nodular goitre. *Best Pract Res Clin Endocrinol Metab* [Internet]. 2014 [cited 2021 Nov 20];28(4):507–518. Available from: <https://pubmed.ncbi.nlm.nih.gov/25047202/>
  55. Hurtado-López LM, Arellano-Montaña S, Torres-Acosta EM, et al. Combined use of fine-needle aspiration biopsy, MIBI scans and frozen section biopsy offers the best diagnostic accuracy in the assessment of the hypofunctioning solitary thyroid nodule. *Eur J Nucl Med Mol Imaging* [Internet]. 2004 [cited 2023 Oct 23];31(9):1273–1279. Available from: <https://pubmed.ncbi.nlm.nih.gov/15133637/>
  56. Giovanella L, Campenni A, Treglia G, et al. Molecular imaging with (99m)Tc-MIBI and molecular testing for mutations in differentiating benign from malignant follicular neoplasm: a prospective comparison. *Eur J Nucl Med Mol Imaging* [Internet]. 2016 [cited 2021 Nov 20];43(6):1018–1026. Available from: <https://pubmed.ncbi.nlm.nih.gov/26695504/>
  57. Campenni A, Giovanella L, Siracusa M, et al. (99m)Tc-Methoxy-Isobutyl-Isonitrile Scintigraphy Is a Useful Tool for Assessing the Risk of Malignancy in Thyroid Nodules with Indeterminate Fine-Needle Cytology. *Thyroid* [Internet]. 2016 [cited 2021 Nov 20];26:1101–1109. Available from: <https://pubmed.ncbi.nlm.nih.gov/27266385/>
  58. Saggiorato E, Angusti T, Rosas R, et al. 99mTc-MIBI Imaging in the presurgical characterization of thyroid follicular neoplasms: relationship to multidrug resistance protein expression. *J Nucl Med* [Internet]. 2009 [cited 2023 Oct 23];50(11):1785–1793. Available from: <https://pubmed.ncbi.nlm.nih.gov/19837765/>
  59. Hervás Morón A. PET-CT in oncology. *Clin Transl Oncol* [Internet]. 2007 [cited 2023 Oct 23];9(8):473–474. Available from: <https://pubmed.ncbi.nlm.nih.gov/17720648/>
  60. Castellana M, Trimboli P, Piccardo A, et al. Performance of 18 F-FDG PET/CT in Selecting Thyroid Nodules with Indeterminate Fine-Needle Aspiration Cytology for Surgery. A Systematic Review and a Meta-Analysis. *JCM* [Internet]. 2019 [cited 2021 Nov 20];8(9):1333. Available from: <https://pubmed.ncbi.nlm.nih.gov/31466411/>
  61. Vriens D, De Wilt JHW, Van Der Wilt GJ, et al. The role of [18 F]-2-fluoro-2-deoxy-d-glucose-positron emission tomography in thyroid nodules with indeterminate fine-needle aspiration biopsy. *Cancer* [Internet]. 2011 [cited 2021 Nov 20];117(20):4582–4594. Available from: <https://pubmed.ncbi.nlm.nih.gov/21432844/>

62. Wang N, Zhai H, Lu Y. Is fluorine-18 fluorodeoxyglucose positron emission tomography useful for the thyroid nodules with indeterminate fine needle aspiration biopsy? A meta-analysis of the literature. *J Otolaryngol Head Neck Surg* [Internet]. 2013 [cited 2021 Nov 20];42. Available from: <https://pubmed.ncbi.nlm.nih.gov/24228840/>
63. de Koster EJ, de Geus-Oei LF, Brouwers AH, et al. [18F]FDG-PET/CT to prevent futile surgery in indeterminate thyroid nodules: a blinded, randomised controlled multicentre trial. *Eur J Nucl Med Mol Imaging* [Internet]. 2022 [cited 2023 Nov 21];49(6):1970–1984. Available from: <https://pubmed.ncbi.nlm.nih.gov/34981165/>.
- **The authors proved the role of [18F]FDG-PET/CT in preventing futile thyroid surgeries in a large multicenter randomized study.**
64. Giovanella L, Milan L, Piccardo A, et al. Radiomics analysis improves 18FDG PET/CT-based risk stratification of cytologically indeterminate thyroid nodules. *Endocrine* [Internet]. 2022 [cited 2021 Oct 16];75(1):202–210. Available from: <https://link.springer.com/article/10.1007/s12020-021-02856-1>
65. de Koster EJ, Noortman WA, Mostert JM, et al. Quantitative classification and radiomics of [18F]FDG-PET/CT in indeterminate thyroid nodules. *Eur J Nucl Med Mol Imaging* [Internet]. 2022 [cited 2023 Oct 25];49(7):2174–2188. Available from: <https://pubmed.ncbi.nlm.nih.gov/35138444/>
66. Giovanella L, Deandreis D, Vrachimis A, et al. Molecular Imaging and Theragnostics of Thyroid Cancers. *Cancers (Basel)* [Internet]. 2022 [cited 2023 Jan 21];14(5):1272. Available from: <https://pubmed.ncbi.nlm.nih.gov/35267580/>
67. Campenni A, Barbaro D, Guzzo M, et al. Personalized management of differentiated thyroid cancer in real life - practical guidance from a multidisciplinary panel of experts. *Endocrine* [Internet]. 2020 [cited 2023 Apr 5];70:280–291. Available from: <https://pubmed.ncbi.nlm.nih.gov/32772339/>
68. Avram AM, Giovanella L, Greenspan B, et al. SNMMI Procedure Standard/EANM Practice Guideline for Nuclear Medicine Evaluation and Therapy of Differentiated Thyroid Cancer: Abbreviated Version. *J Nucl Med* [Internet]. 2022 [cited 2022 Jun 2];63(6):15N–35N. Available from: <https://pubmed.ncbi.nlm.nih.gov/35649660/>
- **The authors of this international guidelines reviewed and provided recommendations on how to manage molecular imaging and theranostics in patients with thyroid cancer.**
69. Aide N, Heutte N, Rame JP, et al. Clinical relevance of single-photon emission computed tomography/computed tomography of the neck and thorax in postablation (131I) scintigraphy for thyroid cancer. *The Journal of Clinical Endocrinology & Metabolism* [Internet]. 2009 [cited 2021 Nov 20];94(6):2075–2084. Available from: <https://pubmed.ncbi.nlm.nih.gov/19276233/>
70. Avram AM. Radioiodine scintigraphy with SPECT/CT: an important diagnostic tool for thyroid cancer staging and risk stratification. *J Nucl Med* [Internet]. 2012 [cited 2021 Nov 20];53(5):754–764. Available from: <http://www.ncbi.nlm.nih.gov/pubmed/22550280>
71. Barbaro D, Campenni A, Forleo R, et al. False-positive radioiodine uptake after radioiodine treatment in differentiated thyroid cancer. *Endocrine* [Internet]. 2023 [cited 2024 Feb 24];81(1):30–35. Available from: <https://pubmed.ncbi.nlm.nih.gov/36928601/>
72. Haugen BR, Alexander EK, Bible KC, et al. 2015 American Thyroid Association Management Guidelines for Adult Patients with Thyroid Nodules and Differentiated Thyroid Cancer: The American Thyroid Association Guidelines Task Force on Thyroid Nodules and Differentiated Thyroid Cancer. *Thyroid* [Internet]. 2016 [cited 2022 Feb 16];26(1):1–133. Available from: <https://pubmed.ncbi.nlm.nih.gov/26462967/>
73. Giovanella L, Trimboli P, Campenni A, et al. Thyroid and Parathyroid Cancer. In: Neri E Erba A, editors. *Multimodality Imaging and Intervention in Oncology* [Internet]. Cham: Springer; 2023 [cited 2024 Feb 24]. p. 45–79. Available from: [https://link.springer.com/chapter/10.1007/978-3-031-28524-0\\_5](https://link.springer.com/chapter/10.1007/978-3-031-28524-0_5)
74. Avram AM, Esfandiari NH, Wong KK. Preablation 131-I scans with SPECT/CT contribute to thyroid cancer risk stratification and 131-I therapy planning. *J Clin Endocrinol Metab* [Internet]. 2015 [cited 2022 Jun 19];100(5):1895–1902. Available from: <https://pubmed.ncbi.nlm.nih.gov/25734251/>
75. Avram AM, Lm FG, Frey KA, et al. Preablation 131-I scans with SPECT/CT in postoperative thyroid cancer patients: what is the impact on staging?. *The Journal of Clinical Endocrinology & Metabolism* [Internet]. 2013 [cited 2021 Nov 20];98(3):1163–1171. Available from: <https://pubmed.ncbi.nlm.nih.gov/23430789/>
76. Spanu A, Solinas ME, Chessa F, et al. 131I SPECT/CT in the follow-up of differentiated thyroid carcinoma: incremental value versus planar imaging. *J Nucl Med* [Internet]. 2009 [cited 2024 Feb 24];50(2):184–190. Available from: <https://pubmed.ncbi.nlm.nih.gov/19164225/>
77. Chen MK, Yasrebi M, Samii J, et al. The utility of I-123 pretherapy scan in I-131 radioiodine therapy for thyroid cancer. *Thyroid: offic j Am Thyroid Association* [Internet]. 2012 [cited 2021 Nov 21];22(3):304–309. Available from: <https://pubmed.ncbi.nlm.nih.gov/22300251/>
78. Song H, Mosci C, Akatsu H, et al. Diagnostic 123I Whole Body Scan Prior to Ablation of Thyroid Remnant in Patients With Papillary Thyroid Cancer: Implications for Clinical Management. *Clin Nucl Med* [Internet]. 2018 [cited 2021 Nov 21];43(10):705–709. Available from: <https://pubmed.ncbi.nlm.nih.gov/30153149/>
79. Liu M, Cheng L, Jin Y, et al. Predicting 131I-avidity of metastases from differentiated thyroid cancer using 18F-FDG PET/CT in post-operative patients with elevated thyroglobulin. *Sci Rep* [Internet]. 2018 [cited 2023 Jun 13];8. Available from: <https://pubmed.ncbi.nlm.nih.gov/29531251/>
80. Avram AM, Dewaraja YK. Thyroid Cancer Radiotheragnostics: the case for activity adjusted 131 I therapy. *Clin Transl Imaging* [Internet]. 2018 [cited 2021 Nov 20];6(5):335–346. Available from: <https://pubmed.ncbi.nlm.nih.gov/30911535/>
81. Barwick T, Murray I, Megadmi H, et al. Single photon emission computed tomography (SPECT)/computed tomography using iodine-123 in patients with differentiated thyroid cancer: additional value over whole body planar imaging and SPECT. *Eur J Endocrinol* [Internet]. 2010 [cited 2023 Nov 15];162(6):1131–1139. Available from: <https://pubmed.ncbi.nlm.nih.gov/20212015/>
82. Campenni A, Ruggeri RM, Siracusa M, et al. Thyroglobulin Value Predict Iodine-123 Imaging Result in Differentiated Thyroid Cancer Patients. *Cancers (Basel)* [Internet]. 2023 [cited 2023 Nov 14];15(8):2242. Available from: <https://pubmed.ncbi.nlm.nih.gov/37190170/>
83. Campenni A, Ruggeri RM, Siracusa M, et al. Isthmus topography is a risk factor for persistent disease in patients with differentiated thyroid cancer. *Eur J Endocrinol* [Internet]. 2021 [cited 2023 Jan 21];185(3):397–404. Available from: <https://pubmed.ncbi.nlm.nih.gov/34232125/>
84. Banerjee M, Wiebel JL, Guo C, et al. Use of imaging tests after primary treatment of thyroid cancer in the United States: population based retrospective cohort study evaluating death and recurrence. *BMJ* [Internet]. 2016 [cited 2021 Nov 21];354. Available from: <https://pubmed.ncbi.nlm.nih.gov/27443325/>
85. Gulec SA, Kuker RA, Goryawala M, et al. 124 I PET/CT in patients with differentiated thyroid cancer: clinical and quantitative image analysis. *Thyroid: offic j Am Thyroid Association* [Internet]. 2016 [cited 2024 Feb 24];26(3):441–448. Available from: <https://pubmed.ncbi.nlm.nih.gov/26857905/>
86. Santhanam P, Taieb D, Solnes L, et al. Utility of I-124 PET/CT in identifying radioiodine avid lesions in differentiated thyroid cancer: a systematic review and meta-analysis. *Clin Endocrinol (Oxf)* [Internet]. 2017 [cited 2021 Nov 20];86(5):645–651. Available from: <https://pubmed.ncbi.nlm.nih.gov/28160320/>
87. Albano D, Dondi F, Bellini P, et al. Biomarkers and Molecular Imaging in Postoperative DTC Management. In: Giovanella L, editor. *Integrated Diagnostics and Theragnostics of Thyroid Diseases* [Internet]. Cham: Springer; 2023 [cited 2024 Feb 24]. p. 129–142.

- Available from: [https://link.springer.com/chapter/10.1007/978-3-031-35213-3\\_8](https://link.springer.com/chapter/10.1007/978-3-031-35213-3_8)
88. Sgouros G, Kolbert KS, Sheikh A, et al. Patient-Specific Dosimetry for <sup>131</sup>I Thyroid Cancer Therapy Using 124I PET and 3-Dimensional-Internal Dosimetry (3D-ID) Software. *J Nucl Med*. 2004;45:1366–1372.
  89. Wierts R, Brans B, Havekes B, et al. Dose–Response Relationship in Differentiated Thyroid Cancer Patients Undergoing Radioiodine Treatment Assessed by Means of 124 I PET/CT. *J Nucl Med* [Internet]. 2016 [cited 2024 Feb 24];57(7):1027–1032. Available from: <https://pubmed.ncbi.nlm.nih.gov/26917706/>
  90. Freudenberg LS, Jentzen W, Petrich T, et al. Lesion dose in differentiated thyroid carcinoma metastases after rhTSH or thyroid hormone withdrawal: 124I PET/CT dosimetric comparisons. *Eur J Nucl Med Mol Imaging* [Internet]. 2010 [cited 2023 Mar 23];37(12):2267–2276. Available from: <https://pubmed.ncbi.nlm.nih.gov/20661558/>
  91. Jentzen W, Verschure F, Van Zon A, et al. 124I PET Assessment of Response of Bone Metastases to Initial Radioiodine Treatment of Differentiated Thyroid Cancer. *J Nucl Med* [Internet]. 2016 [cited 2021 Nov 21];57(10):1499–1504. Available from: <https://pubmed.ncbi.nlm.nih.gov/27199362/>
  92. Miller ME, Chen Q, Elashoff D, et al. Positron emission tomography and positron emission tomography-CT evaluation for recurrent papillary thyroid carcinoma: meta-analysis and literature review. *Head Neck* [Internet]. 2011 [cited 2021 Nov 20];33(4):562–565. Available from: <https://pubmed.ncbi.nlm.nih.gov/20665734/>
  93. Schütz F, Lautenschläger C, Lorenz K, et al. Positron Emission Tomography (PET) and PET/CT in Thyroid Cancer: A Systematic Review and Meta-Analysis. *Eur Thyroid J* [Internet]. 2018 [cited 2021 Nov 20];7(1):13–20. Available from: <https://pubmed.ncbi.nlm.nih.gov/29594049/>
  94. Kim SJ, Lee SW, Pak K, et al. Diagnostic performance of PET in thyroid cancer with elevated anti-Tg Ab. *Endocr Relat Cancer* [Internet]. 2018 [cited 2021 Nov 20];25(6):643–652. Available from: <https://pubmed.ncbi.nlm.nih.gov/29559552/>
  95. Leboulleux S, Schroeder PR, Busaidy NL, et al. Assessment of the incremental value of recombinant thyrotropin stimulation before 2-[<sup>18</sup>F]-Fluoro-2-deoxy-D-glucose positron emission tomography/computed tomography imaging to localize residual differentiated thyroid cancer. *J Clin Endocrinol Metab* [Internet]. 2009 [cited 2023 Jun 8];94(4):1310–1316. Available from: <https://pubmed.ncbi.nlm.nih.gov/19158200/>
  96. Giovanella L, Trimboli P, Verburg FA, et al. Thyroglobulin levels and thyroglobulin doubling time independently predict a positive <sup>18</sup>F-FDG PET/CT scan in patients with biochemical recurrence of differentiated thyroid carcinoma. *Eur J Nucl Med Mol Imaging* [Internet]. 2013 [cited 2023 Aug 14];40(6):874–880. Available from: <https://pubmed.ncbi.nlm.nih.gov/23463330/>
  97. Treglia G, Goichot B, Giovanella L, et al. Prognostic and predictive value of nuclear imaging in endocrine oncology. *Endocrine* [Internet]. 2020 [cited 2023 May 6];67(1):9–19. Available from: <https://pubmed.ncbi.nlm.nih.gov/31734779/>
  98. Petranović Ovčariček P, Campenni A, de Keizer B, et al. Molecular Theranostics in Radioiodine-Refractory Differentiated Thyroid Cancer. *Cancers (Basel)* [Internet]. 2023 [cited 2023 Nov 14];15. Available from 17):4290. Available from: <https://pubmed.ncbi.nlm.nih.gov/37686566/>.
    - **Comprehensive review of the literature on theranostics in radioiodine-refractory differentiated thyroid cancer.**
  99. Deandreis D, Al Ghuzlan A, Leboulleux S, et al. Do histological, immunohistochemical, and metabolic (radioiodine and fluorideoxyglucose uptakes) patterns of metastatic thyroid cancer correlate with patient outcome?. *Endocr Relat Cancer* [Internet]. 2011 [cited 2021 Nov 21];18(1):159–169. Available from: <https://pubmed.ncbi.nlm.nih.gov/21118976/>
  100. Wells SA, Asa SL, Dralle H, et al. Revised American thyroid association guidelines for the management of medullary thyroid carcinoma. *Thyroid: Offic J Am Thyroid Association*. 2015;25(6):567–610. doi: 10.1089/thy.2014.0335
  101. Rasul S, Hartenbach S, Rebhan K, et al. [<sup>18</sup>F]DOPA PET/ceCT in diagnosis and staging of primary medullary thyroid carcinoma prior to surgery. *Eur J Nucl Med Mol Imaging* [Internet]. 2018 [cited 2021 Nov 21];45(12):2159. Available from: <https://pubmed.ncbi.nlm.nih.gov/3182401/>
  102. Cetani F, Marcocci C, Torregrossa L, et al. Atypical parathyroid adenomas: challenging lesions in the differential diagnosis of endocrine tumors. *Endocr Relat Cancer*. 2019;26(7):R441–R464. doi: 10.1530/ERC-19-0135
  103. Fraser WD. Hyperparathyroidism. *Lancet* [Internet]. 2009 [cited 2019 Oct 28];374(9684):145–158. Available from: <http://www.ncbi.nlm.nih.gov/pubmed/19595349>
  104. Yeh MW, Ituarte PHG, Zhou HC, et al. Incidence and prevalence of primary hyperparathyroidism in a racially mixed population. *J Clin Endocrinol Metab* [Internet]. 2013 [cited 2023 Nov 24];98(3):1122–1129. Available from: <https://pubmed.ncbi.nlm.nih.gov/23418315/>
  105. Silverberg SJ, Lewiecki EM, Mosekilde L, et al. Presentation of asymptomatic primary hyperparathyroidism: proceedings of the third international workshop. *J Clin Endocrinol Metab*. 2009;94(2):351–365. doi: 10.1210/jc.2008-1760
  106. Bilezikian JP, Bandeira L, Khan A, et al. Hyperparathyroidism. *Lancet*. 2018;391(10116):168–178. doi: 10.1016/S0140-6736(17)31430-7
  107. Phitayakorn R, McHenry CR. Incidence and location of ectopic abnormal parathyroid glands. *Am J Surg*. 2006;191(3):418–423. doi: 10.1016/j.amjsurg.2005.10.049
  108. Akerström G, Malmaeus J, Bergström R. Surgical anatomy of human parathyroid glands. *Surgery*. 1984;95(1):14–21.
  109. Wang C. The anatomic basis of parathyroid surgery. *Ann Surg* [Internet]. 1976 [cited 2019 Nov 30];183(3):271–275. Available from: <http://www.ncbi.nlm.nih.gov/pubmed/1259483>
  110. Duan K, Gomez Hernandez K, Mete O. Clinicopathological correlates of hyperparathyroidism. *J Clin Pathol*. 2015;68(10):771–787. doi: 10.1136/jclinpath-2015-203186
  111. Singh Ospina NM, Rodriguez-Gutierrez R, Maraka S, et al. Outcomes of Parathyroidectomy in Patients with Primary Hyperparathyroidism: A Systematic Review and Meta-analysis. *World J Surg* [Internet]. 2016 [cited 2020 Aug 3];40:2359–2377. Available from: <http://www.ncbi.nlm.nih.gov/pubmed/27094563>
  112. Bilezikian JP, Brandi ML, Eastell R, et al. Guidelines for the management of asymptomatic primary hyperparathyroidism: summary statement from the Fourth International Workshop. *J Clin Endocrinol Metab*. 2014;99(10):3561–3569. doi: 10.1210/jc.2014-1413
  113. Udelsman R, Lin Z, Donovan P. The superiority of minimally invasive parathyroidectomy based on 1650 consecutive patients with primary hyperparathyroidism. *Ann Surg*. 2011;253(3):585–591. doi: 10.1097/SLA.0b013e318208fed9
  114. Udelsman R. Six hundred fifty-six consecutive explorations for primary hyperparathyroidism. *Ann Surg*. 2002;235(5):665. doi: 10.1097/0000658-200205000-00008
  115. Jinih M, O’Connell E, O’Leary DP, et al. Focused Versus Bilateral Parathyroid Exploration for Primary Hyperparathyroidism: A Systematic Review and Meta-analysis. *Ann Surg Oncol* [Internet]. 2017 [cited 2023 Dec 2];24(7):1924–1934. Available from: <https://pubmed.ncbi.nlm.nih.gov/27896505/>
  116. Wilhelm SM, Wang TS, Ruan DT, et al. The American Association of Endocrine Surgeons Guidelines for Definitive Management of Primary Hyperparathyroidism. *JAMA Surg* [Internet]. 2016 [cited 2019 Dec 1];151(10):959–968. Available from: <http://www.ncbi.nlm.nih.gov/pubmed/27532368>
  117. Hayakawa N, Nakamoto Y, Kurihara K, et al. A comparison between <sup>11</sup>C-methionine PET/CT and MIBI SPECT/CT for localization of parathyroid adenomas/hyperplasia. *Nucl Med Commun*. 2015;36(1):53–59. doi: 10.1097/MNM.0000000000000216
  118. Petranović Ovčariček P, Giovanella L, Carrió Gasset I, et al. The EANM practice guidelines for parathyroid imaging. *Eur J Nucl Med Mol Imaging* [Internet]. 2021 [cited 2022 Jan 24];48(9):2801–2822. Available from: <https://pubmed.ncbi.nlm.nih.gov/33839893/>

- **Updated EANM guideline dedicated to parathyroid imaging, including the role of new technologies.**
- 119. Castellana M, Virili C, Palermo A, et al. Primary hyperparathyroidism with surgical indication and negative or equivocal scintigraphy: safety and reliability of PTH washout. A systematic review and meta-analysis. *Eur J Endocrinol.* 2019;181(3):245–253. doi: 10.1530/EJE-19-0160
- 120. Treglia G, Sadeghi R, Schalin-Jäntti C, et al. Detection rate of <sup>99m</sup>Tc-MIBI single photon emission computed tomography (SPECT)/CT in preoperative planning for patients with primary hyperparathyroidism: A meta-analysis. *Head & Neck* [Internet]. 2016 [cited 2019 Nov 7];38(S1):E2159–E2172. doi: <http://doi.org/10.1002/hed.24027>
- 121. Medas F, Erdas E, Longheu A, et al. Retrospective evaluation of the pre- and postoperative factors influencing the sensitivity of localization studies in primary hyperparathyroidism. *Int J Surg.* 2016;25:82–87. doi: 10.1016/j.ijsu.2015.11.045
- 122. Nichols KJ, Tomas MB, Tronco GG, et al. Sestamibi parathyroid scintigraphy in multigland disease. *Nucl Med Commun.* 2012;33(1):43–50. doi: 10.1097/MNM.0b013e32834bfeb1
- 123. Krakauer M, Wieslander B, Myschetzky PS, et al. A prospective comparative study of parathyroid dual-phase scintigraphy, dual-isotope subtraction scintigraphy, 4D-CT, and ultrasonography in primary hyperparathyroidism. *Clin Nucl Med.* 2016;41(2):93–100. doi: 10.1097/RLU.0000000000000988
- 124. Woods A-M, Bolster AA, Han S, et al. Dual-isotope subtraction SPECT-CT in parathyroid localization. *Nucl Med Commun* [Internet]. 2017 [cited 2019 Dec 5];38(12):1047–1054. Available from: <http://www.ncbi.nlm.nih.gov/pubmed/28984813>
- 125. Kunstman JW, Kirsch JD, Mahajan A, et al. Parathyroid localization and implications for clinical management. *J Clin Endocrinol Metab.* 2013;98(3):902–912. doi: 10.1210/jc.2012-3168
- 126. Palestro CJ, Tomas MB, Tronco GG. Radionuclide imaging of the parathyroid glands. *Semin Nucl Med.* 2005;35(4):266–276. doi: 10.1053/j.semnuclmed.2005.06.001
- 127. Ishibashi M, Nishida H, Hiromatsu Y, et al. Comparison of technetium-99m-MIBI, technetium-99m-tetrofosmin, ultrasound and MRI for localization of abnormal parathyroid glands. *J Nucl Med.* 1998;39(2):320–324.
- 128. Wakamatsu H, Noguchi S, Yamashita H, et al. Technetium-99m tetrofosmin for parathyroid scintigraphy: a direct comparison with <sup>99m</sup>Tc-MIBI, 201TI, MRI and US. *Eur J Nucl Med.* 2001;28(12):1817–1827. doi: 10.1007/s002590100627
- 129. Petranović Ovčariček P, Giovanella L, Hindie E, et al. An essential practice summary of the new EANM guidelines for parathyroid imaging. *Q J Nucl Med Mol Imaging* [Internet]. 2022 [cited 2023 Nov 27];66(2):93–103. Available from: <https://pubmed.ncbi.nlm.nih.gov/35166093/>
- 130. Treglia G, Piccardo A, Imperiale A, et al. Diagnostic performance of choline PET for detection of hyperfunctioning parathyroid glands in hyperparathyroidism: a systematic review and meta-analysis. *Eur J Nucl Med Mol Imaging.* 2019;46(3):751–765. doi: 10.1007/s00259-018-4123-z
- 131. Whitman J, Allen IE, Bergsland EK, et al. Assessment and Comparison of 18 F-Fluorocholine PET and <sup>99m</sup>Tc-Sestamibi Scans in Identifying Parathyroid Adenomas: A Metaanalysis. *J Nucl Med* [Internet]. 2021 [cited 2021 Jan 16]; Available from 62 (9):1285–1291. Available from: <http://jnm.snmjournals.org/lookup/doi/10.2967/jnumed.120.257303>
- 132. Giovanella L, Bacigalupo L, Treglia G, et al. Will 18F-fluorocholine PET/CT replace other methods of preoperative parathyroid imaging?. *Endocrine* [Internet]. 2021 [cited 2021 Apr 9];71(2):285–297. Available from: <http://www.ncbi.nlm.nih.gov/pubmed/32892309>
- 133. López-Mora DA, Sizova M, Estorch M, et al. Superior performance of 18F-fluorocholine digital PET/CT in the detection of parathyroid adenomas. *Eur J Nucl Med Mol Imaging.* 2020;47(3):572–578. doi: 10.1007/s00259-020-04680-7
- 134. Imperiale A, Taieb D, Hindie E. 18F-Fluorocholine PET/CT as a second line nuclear imaging technique before surgery for primary hyperparathyroidism. *Eur J Nucl Med Mol Imaging.* 2018;45(4):654–657. doi: 10.1007/s00259-017-3920-0
- 135. Piccardo A, Bottoni G, Boccalatte LA, et al. Head-to-head comparison among 18 F-choline PET/CT, 4D contrast-enhanced CT, and 18 F-choline PET/4D contrast-enhanced CT in the detection of hyperfunctioning parathyroid glands: a systematic review and meta-analysis. *Endocrine* [Internet]. 2021 [cited 2022 Jan 23];74(2):404–412. Available from: <https://pubmed.ncbi.nlm.nih.gov/34173158/>
- 136. Kluijfhout WP, Pasternak JD, Gosnell JE, et al. <sup>18</sup>F fluorocholine PET/MR imaging in patients with primary hyperparathyroidism and inconclusive conventional imaging: a prospective Pilot study. *Radiology.* 2017;284(2):460–467. doi: 10.1148/radiol.2016160768
- 137. Noltes M, Rotstein L, Eskander A, et al. 18F-fluorocholine PET/MRI versus ultrasound and sestamibi for the localization of parathyroid adenomas. *Langenbecks Arch Surg* [Internet]. 2023 [cited 2023 Nov 23];408. Available from 1). Available from: <https://pubmed.ncbi.nlm.nih.gov/37079138/>
- 138. Huellner MW, Aberle S, Sah B-R, et al. Visualization of Parathyroid Hyperplasia Using 18F-Fluorocholine PET/MR in a Patient With Secondary Hyperparathyroidism. *Clin Nucl Med* [Internet]. 2016 [cited 2020 Aug 3];41(3):e159–61. Available from: <http://www.ncbi.nlm.nih.gov/pubmed/26462047>
- 139. Huber GF, Hüllner M, Schmid C, et al. Benefit of 18F-fluorocholine PET imaging in parathyroid surgery. *Eur Radiol* [Internet]. 2018 [cited 2020 Aug 4];28(6):2700–2707. Available from: <http://www.ncbi.nlm.nih.gov/pubmed/29372312>
- 140. Alharbi AA, Alshehri FM, Albatly AA, et al. [18F]Fluorocholine Uptake of Parathyroid Adenoma Is Correlated with Parathyroid Hormone Level. *Mol Imaging Biol* [Internet]. 2018 [cited 2020 Aug 4];20(5):857–867. Available from: <http://www.ncbi.nlm.nih.gov/pubmed/29508264>
- 141. Parvianin A, Martin-Macintosh EL, Goenka AH, et al. <sup>11</sup>C-Choline PET/CT for Detection and Localization of Parathyroid Adenomas. *Am J Roentgenol* [Internet]. 2018 [cited 2019 Nov 8];210(2):418–422. Available from: <https://www.ajronline.org/doi/10.2214/AJR.17.18312>
- 142. Noltes ME, Kruijff S, Jansen L, et al. A retrospective analysis of the diagnostic performance of 11C-choline PET/CT for detection of hyperfunctioning parathyroid glands after prior negative or discordant imaging in primary hyperparathyroidism. *EJNMMI Res* 2021 [Internet]. 2021 [cited 2021 Sep 14];11(1):1–9. Available from: <https://ejnmires.springeropen.com/articles/10.1186/s13550-021-00778-7>
- 143. Otto D, Boerner AR, Hofmann M, et al. Pre-operative localisation of hyperfunctional parathyroid tissue with 11C-methionine PET. *Eur J Nucl Med Mol Imaging.* 2004;31(10):1405–1412. doi: 10.1007/s00259-004-1610-1
- 144. Kluijfhout WP, Pasternak JD, Drake FT, et al. Use of PET tracers for parathyroid localization: a systematic review and meta-analysis. *Langenbecks Arch Surg.* 2016;401(7):925–935. doi: 10.1007/s00423-016-1425-0
- 145. Bioletto F, Barale M, Parasiliti-Caprino M, et al. Comparison of the diagnostic accuracy of 18F-Fluorocholine PET and 11C-Methionine PET for parathyroid localization in primary hyperparathyroidism: a systematic review and meta-analysis. *Eur J Endocrinol* [Internet]. 2021 [cited 2022 Jan 23];185(1):109–120. Available from: <https://pubmed.ncbi.nlm.nih.gov/33886494/>
- 146. Alabed YZ, Rakheja R, Novales-Diaz JA, et al. Recurrent parathyroid carcinoma appearing as FDG negative but MIBI positive. *Clin Nucl Med.* 2014;39(7):e362–4. doi: 10.1097/RLU.0000000000000357
- 147. Kim SS, Jeon YK, Lee SH, et al. Distant subcutaneous recurrence of a parathyroid carcinoma: abnormal uptakes in the <sup>99m</sup>Tc-sestamibi scan and 18F-FDG PET/CT imaging. *Korean J Intern Med.* 2014;29(3):383. doi: 10.3904/kjim.2014.29.3.383
- 148. Cao C, Dou C, Chen F, et al. An unusual mediastinal parathyroid carcinoma coproducing PTH and PTHrP: a case report. *Oncol Lett.* 2016;11(6):4113–4116. doi: 10.3892/ol.2016.4548
- 149. Singh P, Vadi SK, Saikia UN, et al. Minimally invasive parathyroid carcinoma—A missing entity between parathyroid adenoma and carcinoma: Scintigraphic and histological features. *Clin Endocrinol (Oxf).* 2019;91(6):842–850. doi: 10.1111/cen.14088

150. Hacıyanlı M, Oruk G, Ucarsoy AA, et al. Multiglandular parathyroid carcinoma: case report and review of the literature. *Endocr Pract.* 2011;17(4):e79–83. doi: [10.4158/EP11037.CRR](https://doi.org/10.4158/EP11037.CRR)
151. Ferraro V, Sgaramella LI, Di Meo G, et al. Current concepts in parathyroid carcinoma: a single Centre experience. *BMC Endocr Disord.* 2019;19(S1):46. doi: [10.1186/s12902-019-0368-1](https://doi.org/10.1186/s12902-019-0368-1)
152. Zhang M, Sun L, Rui W, et al. Semi-quantitative analysis of <sup>99m</sup>Tc-sestamibi retention level for preoperative differential diagnosis of parathyroid carcinoma. *Quant Imaging Med Surg.* 2019;9(8):1394–1401. doi: [10.21037/qims.2019.07.02](https://doi.org/10.21037/qims.2019.07.02)
153. Morand GB, Rupp NJ, Huellner MW, et al. Transnasal-Transpterygoid Endoscopic Removal of an <sup>18</sup>F-Choline-Avid parathyroid carcinoma metastasis in the Skull Base. *JAMA Otolaryngology–Head & Neck Surg.* 2019;145(10):978. doi: [10.1001/jamaoto.2019.2352](https://doi.org/10.1001/jamaoto.2019.2352)
154. Deandreis D, Terroir M, Al Ghuzlan A, et al. <sup>18</sup>Fluorocholine PET/CT in parathyroid carcinoma: a new tool for disease staging? *Eur J Nucl Med Mol Imaging.* 2015;42(12):1941–1942. doi: [10.1007/s00259-015-3130-6](https://doi.org/10.1007/s00259-015-3130-6)
155. Hatzl M, Röper-Kelmayr JC, Fellner FA, et al. <sup>18</sup>F-Fluorocholine, <sup>18</sup>F-FDG, and <sup>18</sup>F-Fluoroethyl tyrosine PET/CT in parathyroid cancer. *Clin Nucl Med.* 2017;42(6):448–450. doi: [10.1097/RLU.0000000000001652](https://doi.org/10.1097/RLU.0000000000001652)
156. Rodrigo JP, Hernandez-Prera JC, Randolph GW, et al. Parathyroid cancer: An update. *Cancer Treat Rev.* 2020;86:102012. doi: [10.1016/j.ctrv.2020.102012](https://doi.org/10.1016/j.ctrv.2020.102012)